

# Route, mechanism, and implications of proton import during $\text{Na}^+/\text{K}^+$ exchange by native $\text{Na}^+/\text{K}^+$ -ATPase pumps

Natasia Vedovato and David C. Gadsby

The Laboratory of Cardiac/Membrane Physiology, The Rockefeller University, New York, NY 10065

A single  $\text{Na}^+/\text{K}^+$ -ATPase pumps three  $\text{Na}^+$  outwards and two  $\text{K}^+$  inwards by alternately exposing ion-binding sites to opposite sides of the membrane in a conformational sequence coupled to pump autophosphorylation from ATP and auto-dephosphorylation. The larger flow of  $\text{Na}^+$  than  $\text{K}^+$  generates outward current across the cell membrane. Less well understood is the ability of  $\text{Na}^+/\text{K}^+$  pumps to generate an inward current of protons. Originally noted in pumps deprived of external  $\text{K}^+$  and  $\text{Na}^+$  ions, as inward current at negative membrane potentials that becomes amplified when external pH is lowered, this proton current is generally viewed as an artifact of those unnatural conditions. We demonstrate here that this inward current also flows at physiological  $\text{K}^+$  and  $\text{Na}^+$  concentrations. We show that protons exploit ready reversibility of conformational changes associated with extracellular  $\text{Na}^+$  release from phosphorylated  $\text{Na}^+/\text{K}^+$  pumps. Reversal of a subset of these transitions allows an extracellular proton to bind an acidic side chain and to be subsequently released to the cytoplasm. This back-step of phosphorylated  $\text{Na}^+/\text{K}^+$  pumps that enables proton import is not required for completion of the 3  $\text{Na}^+$ /2  $\text{K}^+$  transport cycle. However, the back-step occurs readily during  $\text{Na}^+/\text{K}^+$  transport when external  $\text{K}^+$  ion binding and occlusion are delayed, and it occurs more frequently when lowered extracellular pH raises the probability of protonation of the externally accessible carboxylate side chain. The proton route passes through the  $\text{Na}^+$ -selective binding site III and is distinct from the principal pathway traversed by the majority of transported  $\text{Na}^+$  and  $\text{K}^+$  ions that passes through binding site II. The inferred occurrence of  $\text{Na}^+/\text{K}^+$  exchange and  $\text{H}^+$  import during the same conformational cycle of a single molecule identifies the  $\text{Na}^+/\text{K}^+$  pump as a hybrid transporter. Whether  $\text{Na}^+/\text{K}^+$  pump-mediated proton inflow may have any physiological or pathophysiological significance remains to be clarified.

## INTRODUCTION

$\text{Na}^+/\text{K}^+$ -ATPase pumps expel three  $\text{Na}^+$  ions and import two  $\text{K}^+$  ions for each ATP hydrolyzed, generating the ion gradients across the membrane that are essential to the life of all animal cells. Each transport cycle comprises a sequence of conformational transitions that permit extracellular  $\text{K}^+$  ions to access the binding sites in phosphorylated pumps (E2P conformations; Fig. 1) and cytoplasmic  $\text{Na}^+$  ions to access the sites after dephosphorylation (E1 conformations; Fig. 1). Binding of the third  $\text{Na}^+$  ion triggers autophosphorylation, and binding of the second  $\text{K}^+$  ion prompts auto-dephosphorylation. This coupling of alternating ion access to ATP hydrolysis ensures forward, energetically uphill, progress of the  $\text{Na}^+/\text{K}^+$  transport cycle. The larger pumped  $\text{Na}^+$  efflux than  $\text{K}^+$  influx constitutes outward current, a direction tending to make the membrane potential more negative. However, because each step in the cycle is reversible (Fig. 1), if the normally transported intracellular  $\text{Na}^+$  and extracellular  $\text{K}^+$  are both scarce, the cycle can run backward, thus synthesizing ATP (Garrahan and Glynn, 1967b) and generating inward, depolarizing current (Bahinski et al., 1988; De Weer et al., 2001).

For a fixed 3  $\text{Na}^+$ /2  $\text{K}^+$  transport stoichiometry (Post and Jolly, 1957; Garrahan and Glynn, 1967a; Rakowski et al., 1989), changes in the magnitude of outward (or inward) pump current report alterations of average turnover rate of the cycle.  $\text{Na}^+/\text{K}^+$  pump current is conveniently measured as the component of membrane current abolished by specific  $\text{Na}^+/\text{K}^+$ -ATPase inhibitors such as ouabain. During control assays of ouabain-sensitive current under nonpumping conditions,  $\text{Na}^+/\text{K}^+$  pumps stalled by withdrawal of external  $\text{K}^+$  ( $\text{K}^+_{\text{o}}$ ) and  $\text{Na}^+$  ( $\text{Na}^+_{\text{o}}$ ) were observed to conduct a measurable inward current at negative membrane potentials (Rakowski et al., 1991). The inward current became larger at more negative voltages, and larger still as extracellular  $[\text{H}^+]$  was raised, and so was attributed to proton inflow (Efthymiadis et al., 1993). This suggestion was supported by the negative shifts of the current's reversal potential that accompanied the ouabain-sensitive intracellular acidification observed after oocytes were held at negative potentials in pH-6.0 solution for several minutes (Wang and Horisberger, 1995). A link between this proton inflow and the third  $\text{Na}^+$ -binding site was inferred when mutations in a region

Correspondence to David C. Gadsby: [gadsby@rockefeller.edu](mailto:gadsby@rockefeller.edu)

Abbreviations used in this paper: EAAT, excitatory amino acid transporter; MTSET<sup>+</sup>, 2-(trimethylammonium)ethyl MTS; TM, transmembrane.

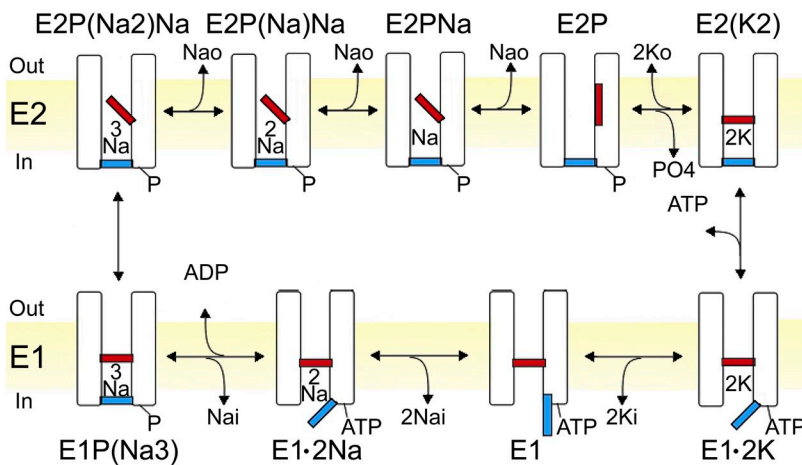


**Figure 1.** The Post-Albers transport cycle (e.g., Post et al., 1972) of the  $\text{Na}^+,\text{K}^+$ -ATPase cartooned as an ion channel with two gates. The gates open strictly alternately to allow access to cation-binding sites from only one side at a time. The extracellular-side gate (red) is closed in all E1 states, and the cytoplasmic-side gate (blue) is closed in E2 states. Parentheses denote occluded ions, and “P” symbolizes the aspartyl-phosphate formed by autophosphorylation of E1 pumps once three cytoplasmic  $\text{Na}^+$  ions have bound.

suggested by homology modeling to be selective for  $\text{Na}^+$  binding (Ogawa and Toyoshima, 2002) diminished both the inward current and inhibition by  $\text{Na}^+$  of outward  $\text{Na}^+/\text{K}^+$  pump current at negative potentials (Li et al., 2006). More recently, the inward current was found to be augmented by mutations at the  $\text{Na}^+/\text{K}^+$  pump’s C terminus (Yaragatupalli et al., 2009; Meier et al., 2010; Poulsen et al., 2010; Vedovato and Gadsby, 2010), and in some instances was further enhanced in the presence of  $\text{Na}^+$ ; these findings reinforced an earlier proposal (Vasilyev et al., 2004) that  $\text{Na}^+$  ions could also flow along what has come to be referred to as the  $\text{Na}^+/\text{K}^+$  pump “leak” pathway (Vasilyev et al., 2004; Yaragatupalli et al., 2009; Meier et al., 2010; Poulsen et al., 2010; Azizan et al., 2013; Nyblom et al., 2013).

We demonstrate here, however, that the inward  $\text{Na}^+/\text{K}^+$  pump-mediated proton current requires neither the absence of external  $\text{K}^+$  or  $\text{Na}^+$  nor extreme negative potentials, and can be observed in native  $\text{Na}^+/\text{K}^+$  pumps at physiological  $\text{K}^+$  and  $\text{Na}^+$  concentrations and resting potentials. Proton inflow is produced by phosphorylated conformations through which each  $\text{Na}^+/\text{K}^+$  pump transits during every  $\text{Na}^+/\text{K}^+$  transport cycle. But whether a proton traverses the  $\text{Na}^+/\text{K}^+$  pump in any given cycle is determined by several factors. When even a small delay in  $\text{Na}^+/\text{K}^+$  pump dephosphorylation postpones completion of the cycle, extracellular protons can exploit rapid reversibility of  $\text{Na}^+$ -releasing transitions among phosphorylated conformations to enter the cell. Protons hop from a protonatable side chain accessible from the extracellular side in one phosphorylated E2 conformation to another protonatable residue with access to the cytoplasm in a kinetically adjacent phosphorylated E2 conformation. By systematic neutralization of carboxylates in the  $\text{Na}^+/\text{K}^+$  pump TM domain, we here identify a glutamate and aspartate, and an intervening tyrosine, as forming the core proton route, which traverses the third  $\text{Na}^+$ -binding site observed in the latest  $\text{Na}^+/\text{K}^+$  pump crystal structures (Kanai et al., 2013; Nyblom et al., 2013).

In corresponding E2 states of the related SERCA  $\text{Ca}^{2+}$ -ATPase, reversible protonation of cation-coordinating carboxylates compensates the charge imbalance that would otherwise attend release of the two transported  $\text{Ca}^{2+}$  ions into the sarcoplasmic/endoplasmic reticulum (Obara et al., 2005). Release of those protons to the cytoplasm in E1 states, before the next  $\text{Ca}^{2+}$  ions bind, results in countertransport of two or three protons each ATPase cycle (Yu et al., 1993). The  $\text{H}^+/\text{K}^+$ -ATPases, the closest relatives of  $\text{Na}^+/\text{K}^+$  pumps, also transport two protons but from the cytoplasm to the cell exterior, analogous to the extrusion of three  $\text{Na}^+$  ions by a  $\text{Na}^+/\text{K}^+$  pump; and, like  $\text{Na}^+/\text{K}^+$  pumps, the  $\text{H}^+/\text{K}^+$ -ATPases countertransport two  $\text{K}^+$  ions. In  $\text{H}^+/\text{K}^+$  pumps, the “third” ion-binding site is modeled to contain the positively charged side chain of a lysine, not found in  $\text{Na}^+/\text{K}^+$  pumps (Poulsen et al., 2010); replacing that lysine by alanine makes the electroneutral  $\text{H}^+/\text{K}^+$  pump become electrogenic (Burnay et al., 2003). But whether proton transport by  $\text{H}^+/\text{K}^+$  pumps occurs by reversible protonation of cation-coordinating carboxylates or by transport of hydronium ions is not yet established (e.g., Law et al., 2008).

The proton inflow through the  $\text{Na}^+/\text{K}^+$  pump is energetically downhill and is not obligatory for completion of the forward  $\text{Na}^+/\text{K}^+$  transport cycle. But we speculate that it might accompany  $\text{Na}^+/\text{K}^+$  pumping at the normal negative resting potentials of neurons, and cardiac and skeletal muscle cells, if extracellular pH were to fall sufficiently, as might occur, for example, during strenuous muscle exercise or cardiac or cerebral ischemia, and does occur in endosomes.

## MATERIALS AND METHODS

### Mutagenesis and expression

Substitutions in the *Xenopus laevis*  $\text{Na}^+,\text{K}^+$ -ATPase  $\alpha 1$  subunit cDNA were introduced using QuickChange (Agilent Technologies) and verified by automated sequencing, as described previously (Reyes and Gadsby, 2006; Takeuchi et al., 2008; Vedovato and Gadsby, 2010). The substitution C113Y (Canessa et al., 1992) rendered the *Xenopus*  $\text{Na}^+,\text{K}^+$ -ATPase  $\alpha 1$  subunit ouabain resistant and insensitive

to extracellular application of hydrophilic, membrane-impermeant MTS reagents; this C113Y construct served as the template for other mutations. After in vitro transcription of cDNA in pSD5 vector, 15–45 ng of wild-type or mutant  $\text{Na}^+/\text{K}^+$ -ATPase  $\alpha 1$  subunit cRNA was coinjected with 5–15 ng of *Xenopus*  $\beta 3$  subunit cRNA into defolliculated *Xenopus* oocytes, which were incubated at 18°C for 2–4 d before recording.

### Solutions

External solutions contained 125 mM NaOH or tetramethylammonium-OH, 120 mM sulfamic acid, 0–30 mM  $\text{K}^+$ -sulfamate, 5 mM BaCl<sub>2</sub>, 1 mM MgCl<sub>2</sub>, 0.5 mM CaCl<sub>2</sub>, plus 1  $\mu\text{M}$  ouabain to inhibit endogenous  $\text{Na}^+/\text{K}^+$  pumps (omitted in experiments to study wild-type *Xenopus*  $\alpha 1/\beta 3$   $\text{Na}^+/\text{K}^+$  pumps), and were buffered to pH 7.6 with 10 mM HEPES or to pH 6.0 with 10 mM Mes; osmolality was 250–260 mosmol/Kg. To inhibit all  $\text{Na}^+/\text{K}^+$  pumps (whether wild type or ouabain resistant), 10 mM ouabain was directly dissolved into the appropriate external solution. 2-(Trimethylammonium)ethyl MTS (MTSET<sup>+</sup>) was diluted from a 100-mM aqueous stock into external solution to a final concentration of 1 mM just before use. A subset of oocytes was injected with 50 nL of 1 mM BeF<sub>X</sub> (1 mM BeSO<sub>4</sub> plus 25 mM NaF) aqueous solution, which was expected to dilute to  $\sim$ 100  $\mu\text{M}$  in the oocyte intracellular volume. Before recording,  $[\text{Na}^+]$  was raised by putting oocytes for  $\geq 2$  h in  $\text{K}^+$ - and  $\text{Ca}^{2+}$ -free solution, containing 95 mM NaOH, 90 mM sulfamic acid, 10 mM TEACl, 0.1 mM EGTA, and 5 mM HEPES, pH 7.6; osmolality was  $\sim$ 210 mosmol/Kg. Pipette (cytoplasmic) solution for outside-out patch recordings contained 125 mM NaOH, 120 mM sulfamic acid, 1 mM MgATP, 1 mM MgCl<sub>2</sub>, 0.1 mM EGTA, 10 mM HEPES, pH 7.4, plus 10  $\mu\text{M}$  ouabain (to avoid palytoxin-induced currents from endogenous  $\text{Na}^+/\text{K}^+$  pumps). Palytoxin (from *Palythoa tuberculosa*; Wako Pure Chemical Industries, Ltd.) was dissolved in aqueous 0.001% wt/vol BSA solution, and the 100- $\mu\text{M}$  stock solution was stored at  $-20^\circ\text{C}$ . Just before use, it was diluted to a final concentration of 100 nM in 125 mM Na<sub>o</sub> solution supplemented with 0.001% BSA and 1 mM Na-borate.

### Electrophysiology

Oocytes expressing wild-type and ouabain-resistant mutant  $\text{Na}^+/\text{K}^+$  pumps were studied at 22–24°C by two-microelectrode voltage clamp, as described previously (Vedovato and Gadsby, 2010). Whole oocyte currents were acquired with an OC-725A amplifier (Warner Instruments) filtered at 1 kHz and sampled at 5 kHz with an 18-bit ITC-18 A/D-D/A board controlled by Patch Master 2.20 software (Instrutech; HEKA). Steady-state currents (and pre-steady-state transient  $\text{Na}^+$  currents in 125 mM Na<sub>o</sub>, 0 K<sub>o</sub>) were elicited with 50-ms voltage steps to potentials between  $-180$  and  $+60$  mV, in increments of 20 mV, from a holding potential of  $-20$  or  $-50$  mV, and were averaged over the last 10 ms of each step.  $\text{Na}^+$  charge-movement quantities,  $\Delta Q$ , were obtained directly as integrals of the ouabain-sensitive transient currents at the  $-20$ -mV holding potential upon termination of each voltage step. Single-exponential fits (beginning 1–3 ms after the start of the step) to the decay time courses of the transient currents elicited by the ON voltage steps gave relaxation rates of the slow components of pump charge movement. Data were analyzed with IgorPro 6 (WaveMetrics) and Origin 7.0 (OriginLab Corporation). C113Y or D935N(C113Y) mutant  $\text{Na}^+/\text{K}^+$  pumps expressed in oocytes were also examined at 22–24°C in outside-out excised patches. Patch current was recorded with an Axopatch 200B amplifier (Molecular Devices), filtered at 500 Hz, and sampled at 5 kHz with a Digidata 1200 A/D-D/A driven by pClamp7 software (Molecular Devices). Palytoxin was applied to outside-out patches held at  $-50$  mV in symmetric 125-mM Na<sub>o</sub> solutions until inward  $\text{Na}^+/\text{K}^+$  pump-channel current reached a steady level, and was then washed out. Data were analyzed with ClampFit (in pClamp 9; Molecular Devices). Results are reported as mean  $\pm$  SEM of  $n$  measurements.

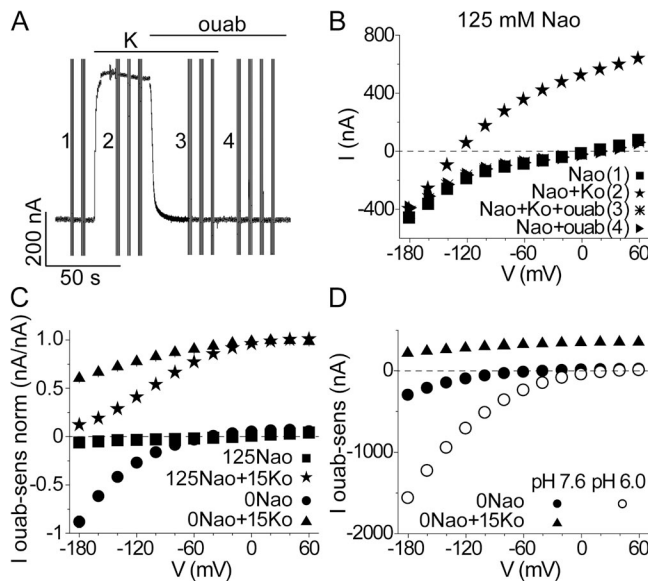
### Online supplemental material

Fig. S1 presents detailed average pump-mediated current–voltage relationships with or without saturating K<sub>o</sub>, in 125 mM Na<sub>o</sub> or 0 mM Na<sub>o</sub>, for E336Q, E788Q, D813N, and D817N mutant  $\text{Na}^+/\text{K}^+$  pumps, with each mutant compared side-by-side with the parent C113Y  $\text{Na}^+/\text{K}^+$  pump (*Xenopus*  $\alpha 1$  subunit numbering throughout). Fig. S2 similarly compares the pump current–voltage relationships of C113Y pumps under all those conditions with those of Y780F, D935N, E963Q, and double D935N/E963Q mutant  $\text{Na}^+/\text{K}^+$  pumps. Fig. S3 summarizes the influence of assorted other mutations (e.g., of TM histidines, of C-terminal basic residues and deletions, and of alternative ouabain-resistance conferring residues) on the ability of lowered extracellular pH (pH<sub>o</sub>) to amplify pump-mediated inward current at large negative potentials, in comparison to the response of C113Y  $\text{Na}^+/\text{K}^+$  pumps. Fig. S4 compares average pump-mediated current–voltage relationships of wild-type *Xenopus*  $\alpha 1/\beta 3$   $\text{Na}^+/\text{K}^+$  pumps with those of C113Y *Xenopus*  $\alpha 1/\beta 3$   $\text{Na}^+/\text{K}^+$  pumps, in 125 mM Na<sub>o</sub>, with 0 or 15 mM K<sub>o</sub>, all at pH<sub>o</sub> 7.6 and at pH<sub>o</sub> 6.0. The online supplemental material is available at <http://www.jgp.org/cgi/content/full/jgp.201311148/DC1>.

## RESULTS

### Outward $\text{Na}^+/\text{K}^+$ transport current

Adding K<sub>o</sub> activates the millions of wild-type  $\alpha 1/\beta 3$  *Xenopus*  $\text{Na}^+/\text{K}^+$  pumps (believed to be the native isoforms; Verrey et al., 1989; Good et al., 1990) overexpressed in a *Xenopus* oocyte with elevated intracellular Na<sub>i</sub>, [Na<sub>i</sub>], eliciting a large outward current that is rapidly abolished by ouabain (Fig. 2 A; for consistency, 10 mM ouabain was used in all experiments regardless of whether wild-type or ouabain-resistant pumps were studied). Voltage steps allow current measurements over a range of membrane potentials with and without ouabain (Fig. 2 B), yielding ouabain-sensitive, i.e.,  $\text{Na}^+/\text{K}^+$  pump-mediated, currents by subtraction (Fig. 2 C). At this saturating, 15 mM, [K<sub>o</sub>] outward pump current approaches the same voltage-independent maximum at positive potentials with 125 mM Na<sub>o</sub> (Fig. 2 C, stars) or without Na<sub>o</sub> (Fig. 2 C, triangles; Nakao and Gadsby, 1989; Vedovato and Gadsby, 2010). This reflects ultimate rate limitation of the forward 3  $\text{Na}^+/\text{2 K}^+$  exchange transport cycle by K<sup>+</sup> deocclusion, E2(K2)  $\rightarrow$  E1 · 2K (Fig. 1; Post et al., 1972; Forbush, 1987a), a step known to be voltage insensitive (Bahinski et al., 1988). The maximal turnover rate of the cycle can be calculated from this maximum current amplitude if the number of functional  $\text{Na}^+/\text{K}^+$  pumps in each oocyte is known. The latter is obtained from the total quantity of charge moved by transient  $\text{Na}^+$  currents in response to voltage steps in 125 mM Na<sub>o</sub> in the absence of K<sub>o</sub> (e.g., Fig. 6, below; Nakao and Gadsby, 1986; Vedovato and Gadsby, 2010). A Boltzmann fit to a plot of Na<sup>+</sup> charge,  $\Delta Q$ , elicited by each step against membrane potential during that step gives total moveable charge,  $Q_{\text{tot}}$ , and steepness,  $z_q$ , and hence equivalent charge moved per pump,  $z_q \cdot e_0$ ; in each oocyte, the number of participating pumps is then determined as  $N_p = Q_{\text{tot}}/z_q \cdot e_0$ . For a presumed 3  $\text{Na}^+/\text{2 K}^+$  transport stoichiometry (Post and Jolly, 1957; Garrahan and Glynn, 1967a; Rakowski et al.,



**Figure 2.** Outward and inward current components in wild-type  $\text{Na}^+/\text{K}^+$  pumps. (A) Current in a single  $\text{Na}^+$ -loaded oocyte overexpressing wild-type  $\alpha 1/\beta 3$  *Xenopus*  $\text{Na}^+/\text{K}^+$ -ATPase pumps, at  $-20$  mV, in  $125\text{-mM Na}^+_{\text{o}}$  solutions. The addition of  $15\text{ mM K}^+_{\text{o}}$  (bar labeled “K”) activated large outward  $3\text{ Na}^+/\text{2 K}^+$  exchange current that was abolished by  $10\text{ mM ouabain}$  (bar labeled “ouab”). Vertical lines are responses to  $50\text{-ms}$  jumps to other potentials. (B) Steady currents from the oocyte in A plotted against voltage for the trials identified by numbers 1–4 in A. (C) Average ouabain-sensitive currents ( $I_{\text{ouab-sens}}$  norm) obtained by subtraction of currents like those in B, at every voltage and presence or absence of  $\text{K}^+_{\text{o}}$ , were normalized to the mean amplitude between  $0$  and  $60$  mV of ouabain-sensitive current at  $15\text{ mM [K}^+_{\text{o}}\text{] in 0 or 125 mM Na}^+_{\text{o}}$ , as appropriate; normalized currents were then averaged across oocytes;  $\pm\text{SEM}$  is visible where larger than the symbols;  $n = 8$  at  $125\text{ mM Na}^+_{\text{o}}$ ;  $n = 5$  at  $0\text{ Na}^+_{\text{o}}$ . In direct comparisons in the same oocyte, maximal outward ouabain-sensitive current at  $15\text{ mM [K}^+_{\text{o}}\text{] and positive voltage is the same in the presence or absence of Na}^+_{\text{o}}$  (Vedovato and Gadsby, 2010). (D) Ouabain-sensitive currents in a representative oocyte at  $0\text{ mM Na}^+_{\text{o}}$ . At  $\text{pH}_o$   $7.6$ , ouabain-sensitive currents in  $15\text{ mM K}^+_{\text{o}}$  (closed triangles) or in  $0\text{ mM K}^+_{\text{o}}$  (closed circles) are like those in C, but upon lowering  $\text{pH}_o$  to  $6.0$  in  $0\text{ mM K}^+_{\text{o}}$  (open circles), inward current at negative potentials increased approximately fivefold.

1989), and thus net movement across the membrane of a single charge per cycle, the turnover rate at any given pump current amplitude,  $I_p$ , at any membrane potential is estimated as  $I_p/N_p \cdot e_0$  or  $I_p \cdot z_q/Q_{\text{tot}}$ . The maximal turnover rate of wild-type  $\alpha 1/\beta 3$  *Xenopus*  $\text{Na}^+/\text{K}^+$  pumps at room temperature is calculated in this way to be  $\sim 45\text{ s}^{-1}$  (compare to Vedovato and Gadsby, 2010).

In the presence of  $\text{Na}^+_{\text{o}}$ , the outward  $\text{Na}^+/\text{K}^+$  pump current declines at negative membrane potentials (Fig. 2 C, stars). This reflects the strong influence of negative voltage to selectively enhance rebinding of extracellularly released  $\text{Na}^+$  to the  $\text{Na}^+$ -specific (Schneeberger and Apell, 2001; Li et al., 2005; Ratheal et al., 2010) site III, which lies deep within the pump (Kanai et al., 2013; Nyblom et al., 2013) partway through the membrane’s electric field. As a result, the apparent affinity for  $\text{Na}^+_{\text{o}}$  is increased relative to that for  $\text{K}^+_{\text{o}}$  at negative voltages (Nakao and

Gadsby, 1989; Gadsby et al., 1993; Sagar and Rakowski, 1994; Vedovato and Gadsby, 2010), allowing bound  $\text{Na}^+$  to more effectively impede  $\text{K}^+_{\text{o}}$  binding. Consequently, dephosphorylation of E2P and formation of the occluded E2( $\text{K}2$ ) state, and hence completion of the  $\text{Na}^+/\text{K}^+$  transport cycle, are all delayed. Accordingly, when  $\text{Na}^+_{\text{o}}$  is absent, the steep diminution of outward  $\text{Na}^+/\text{K}^+$  pump current at negative voltages is greatly attenuated (Fig. 2 C, triangles).

#### Pump-mediated inward proton current

Without  $\text{K}^+_{\text{o}}$  ions to activate  $\text{Na}^+/\text{K}^+$  transport, the wild-type  $\text{Na}^+/\text{K}^+$  pumps generate little steady current at any voltage at  $125\text{ mM Na}^+_{\text{o}}$  (Fig. 2 C, squares). But in the absence of both  $\text{K}^+_{\text{o}}$  and  $\text{Na}^+_{\text{o}}$ , there is an easily measured inward current (Rakowski et al., 1991) that increases steeply at more negative potentials (Fig. 2 C, circles). Upon closer inspection, this inward current is discernible even in  $125\text{ mM Na}^+_{\text{o}}$ , although severalfold smaller (Fig. 2 C, squares vs. circles; see also Figs. 8 B and S4 A, closed squares). Its amplification on lowering external pH ( $\text{pH}_o$ ), whether  $\text{Na}^+_{\text{o}}$  is absent (Fig. 2 D, open circles) or present (see Fig. 8 B), argues that protons carry the current (Efthymiadis et al., 1993; Wang and Horisberger, 1995). Comparison of the size of this inward current with maximal outward  $\text{Na}^+/\text{K}^+$  transport current (representing outflow of  $\sim 45$  positive charges/s through each pump) in the same pumps indicates that, even at  $-180$  mV in  $0\text{ Na}^+_{\text{o}}$  at  $\text{pH}_o$   $6.0$  (Fig. 2 D), the inward current represents inflow of only  $\sim 200$  protons  $\text{s}^{-1}$  per pump. This meager throughput rate could reflect limitation of proton electrodiffusion through a water-filled pore by the low proton concentration, here  $1\text{ }\mu\text{M}$  (DeCoursey, 2003). However, the enthalpic activation energy of the inward current in  $\text{Na}^+/\text{K}^+$  pumps lacking the two C-terminal tyrosines ( $\Delta YY$ ) was found to be very high,  $\sim 140\text{ kJ/mol}$ , identical to that of outward  $\text{Na}^+/\text{K}^+$  transport current in the same pumps (Meier et al., 2010), suggesting that the inward current is rate limited by substantial changes in pump conformation. A plausible conformational mechanism for inward proton transport could be that a protonatable side chain is exposed to extracellular fluid in one  $\text{Na}^+/\text{K}^+$  pump conformation that is in equilibrium with another conformation in which the side chain has cytosolic access (Fig. 3 A); a proton gradient could then drive net proton movement across the membrane. Just such a mechanism has been shown to generate voltage-sensitive proton current in Shaker voltage-gated  $\text{K}^+$  channels in which a histidine had been substituted for one of the voltage-sensor arginines (Starace and Bezanilla, 2001).

#### Two carboxylates and a hydroxyl required for proton inflow

Appropriate candidates for such protonatable residues in the  $\text{Na}^+/\text{K}^+$  pump are six conserved acidic amino

acids (Fig. 3 B) in the transmembrane (TM) domain that have been implicated, or demonstrated to be involved, in coordinating bound K<sup>+</sup> and/or Na<sup>+</sup> ions. Thus, E336 (*Xenopus*  $\alpha 1$  numbering) in TM helix 4 (TM4), E788 in TM5, and D813 and D817 in TM6 are all involved in coordination (directly, or via a water) of K<sup>+</sup> or Na<sup>+</sup> ions in sites I and II in the crystal structures of K<sup>+</sup>-bound (E2 · MgF<sub>4</sub><sup>2-</sup> · 2 K<sup>+</sup>; Morth et al., 2007; Shinoda et al., 2009) or Na<sup>+</sup>-bound (E1 · AlF<sub>4</sub><sup>-</sup> · ADP · 3 Na<sup>+</sup>; Kanai et al., 2013; Nyblom et al., 2013) Na<sup>+</sup>/K<sup>+</sup> pumps. D935 in TM8 contributes to coordination of the Na<sup>+</sup> in site III (Kanai et al., 2013), and E963 in TM9 had previously been linked to a Na<sup>+</sup>-selective binding site by homology modeling (Ogawa and Toyoshima, 2002) and mutagenesis (Li et al., 2005, 2006). To assess a possible role of each of these residues in the proton current, we neutralized them one at a time and then tested whether a pH<sub>o</sub> drop from 7.6 to 6.0 in K<sup>+</sup>-free, Na<sup>+</sup>-free solution caused a large increase in inward current, like that seen in wild-type Na<sup>+</sup>/K<sup>+</sup> pumps in Fig. 2 D. These neutralizing mutations were introduced one at a time into *Xenopus*  $\alpha 1/\beta 3$  Na<sup>+</sup>/K<sup>+</sup> pumps that had been made relatively ouabain resistant by the single  $\alpha 1$ -subunit mutation C113Y (Canessa et al., 1992), so that 10 mM ouabain could be used to obtain mutant pump currents, whereas the continuous presence of 1  $\mu$ M ouabain silenced endogenous *Xenopus* Na<sup>+</sup>/K<sup>+</sup> pumps (e.g., Takeuchi et al., 2008; Vedovato and Gadsby, 2010).

The carboxylate mutants all expressed well, as revealed by the magnitude of pump-mediated transient Na<sup>+</sup> charge movements elicited by voltage steps. We found wild-type-like Na<sup>+</sup>/K<sup>+</sup> outward currents, influenced in

the usual voltage-dependent manner by Na<sup>+</sup><sub>o</sub> (Fig. 2 C), in the ouabain-resistant C113Y parent Na<sup>+</sup>/K<sup>+</sup> pumps (see Vedovato and Gadsby, 2010), and in E788Q (Fig. S1 F; Peluffo et al., 2000; Koenderink et al., 2003) and E963Q (Fig. S2 D; Li et al., 2006) pumps, whereas 15-mM K<sup>+</sup><sub>o</sub>-activated outward currents in D935N (Fig. S2 B) and double D935N/E963Q (Fig. S2 F) mutants failed to saturate at positive voltage and were insensitive to the presence or absence of Na<sup>+</sup><sub>o</sub>. In contrast, outward Na<sup>+</sup>/K<sup>+</sup> transport currents were absent in E336Q and D813N mutants, with or without Na<sup>+</sup><sub>o</sub> (Fig. S1, B and D; Nielsen et al., 1998; Vilse and Andersen, 1998; Koenderink et al., 2003), and present in D817N only at 0 Na<sup>+</sup><sub>o</sub> and elevated (30 mM) K<sup>+</sup><sub>o</sub> (Fig. S1 H).

In K<sup>+</sup><sub>o</sub>-free, Na<sup>+</sup><sub>o</sub>-free solution, inward current at large negative potentials increased severalfold on lowering pH<sub>o</sub> to 6.0 in the ouabain-insensitive background C113Y *Xenopus* Na<sup>+</sup>/K<sup>+</sup> pumps (Fig. 4, A–D and F, black symbols repeated in each graph), just like in wild-type *Xenopus* Na<sup>+</sup>/K<sup>+</sup> pumps (Fig. 2 D). Relatively large inward currents at pH<sub>o</sub> 6.0 were also preserved in E336Q and D813N (Fig. 4 A), and in E788Q and D817N (Fig. 4 B) individual mutant Na<sup>+</sup>/K<sup>+</sup> pumps, but were greatly diminished in D935N (Poulsen et al., 2010) and E963Q (compare to Li et al., 2006) mutants (Fig. 4 C; also in D935C, Fig. S3), and were essentially abrogated in the D935N/E963Q double mutant (Fig. 4 D). Because the residual inward currents in D935N (Fig. 4 C) and D935N/E963Q (Fig. 4 D) pumps are displayed normalized to the observed outward current at positive potentials in those pumps, despite its failure to reach a voltage-insensitive maximum (Fig. S2 B), those currents are overestimates

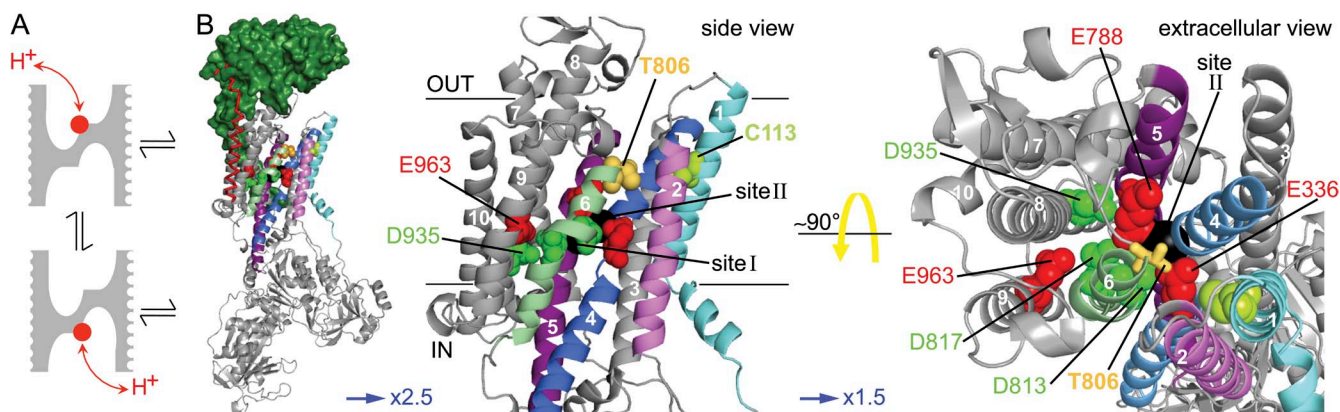


**Figure 3.** Proposed proton transport mechanism and candidate carboxylates. (A) Cartoon of proposed mechanism indicating protonation/deprotonation of a side chain (red circle) with alternate extracellular and cytoplasmic access in kinetically adjacent pump conformations; gray mass represents protein barrier to proton diffusion in the relevant segment of Na<sup>+</sup>/K<sup>+</sup> pump TM domain structure. (B; from left to right) Increasingly magnified (factors indicated by blue arrows) views of *Xenopus*  $\alpha 1/\beta 3$  Na<sup>+</sup>/K<sup>+</sup> pump homology model based on x-ray crystal structure of the K<sup>+</sup>-bound E2 · MgF<sub>4</sub><sup>2-</sup> · Na<sup>+</sup>/K<sup>+</sup>-ATPase (Protein Data Bank accession no. 2ZZE; Shinoda et al., 2009), showing the  $\alpha$  subunit (gray, with 5 of the 10 TM helices colored),  $\beta$  subunit (green surface), and  $\gamma$  subunit (red helix). (Middle and right) Side and top (from extracellular surface) views of the  $\alpha$ -subunit TM domain (helix numbers in white) identifying six candidate carboxylates, three Glu (red spheres) and three Asp (green spheres), at the level of binding sites I and II that contain K<sup>+</sup> ions (black balls); the colored TM helices are: pale blue, TM1; magenta, TM2; blue, TM4; purple, TM5; and green, TM6. Gray, TM3 and TM7–TM10; lime spheres, C113 in TM1; yellow spheres (left) or sticks (right) mark T806 at the top of TM6.

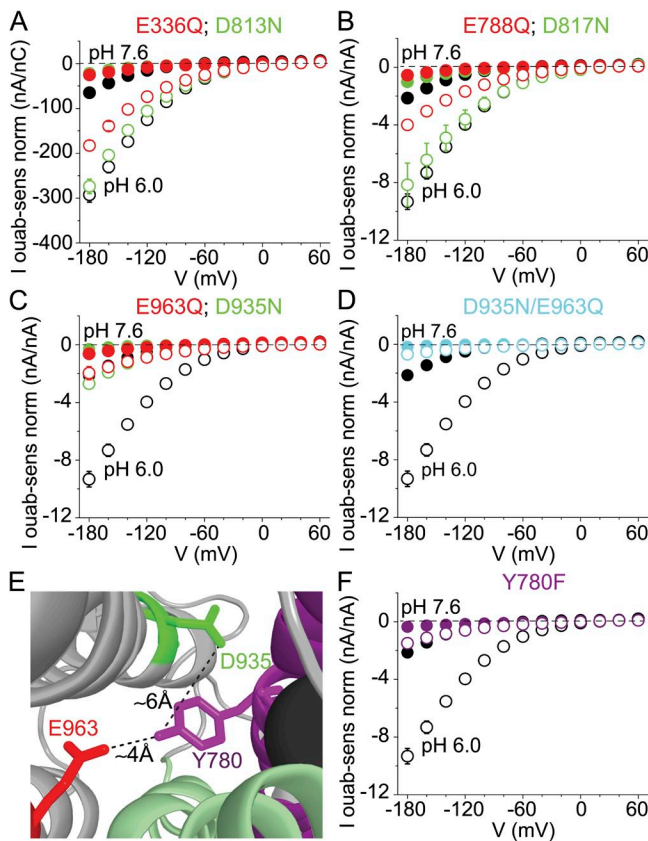


**Figure 4.** External pH sensitivity of ouabain-sensitive inward current in  $0\text{Na}^+$  and  $0\text{K}^+$  after conservative mutation of each candidate residue in partially ouabain-resistant C113Y pumps. Each Glu (red circles) and Asp (green circles) was neutralized, and the inward current response to lowering  $\text{pH}_o$  (open vs. closed circles) was compared with that of the parent C113Y pumps (black circles). For these comparisons, inward current was normalized to maximally  $\text{K}^+$ -activated (10–30 mM  $[\text{K}^+]$ ), ouabain-sensitive outward pump current (Figs. S1 and S2) recorded in the same oocyte, averaged between 0 and +60 mV; because E336Q and D813N pumps lacked  $\text{K}^+$ -activated current (Fig. S1, B and D), inward current was normalized to total pump-mediated  $\text{Na}^+$  charge movement,  $Q_{\text{tot}}$ , in  $0\text{K}^+$ , 125 mM  $\text{Na}^+$  solution (Nakao and Gadsby, 1986; Vasilyev et al., 2004; Meier et al., 2010; Poulsen et al., 2010; Vedovato and Gadsby, 2010) in the same oocyte. Inward current of (A) E336Q ( $n = 3$ ) and D813N ( $n = 6$ ), and of (B) E788Q ( $n = 7$ ) and D817N ( $n = 5$ ), pumps, like that of control C113Y pumps ( $n = 12$ –16), increased substantially on lowering  $\text{pH}_o$  from 7.6 to 6.0; inward current at  $\text{pH}_o$  6.0 and –180 mV in E336Q, D813N, and D817N was >60%, and in E788Q it was 43%, that of C113Y pumps. But inward current of (C) D935N ( $n = 5$ ) and E963Q ( $n = 4$ ) pumps was comparatively small at  $\text{pH}_o$  6.0, and that of (D) D935N/E963Q double mutant (cyan;  $n = 3$ ) pumps was almost absent compared with C113Y pumps ( $n = 16$ ); as  $\text{K}^+$ -activated currents of D935N and D935N/E963Q pumps fail to reach a voltage-independent maximum at positive potentials (Figs. 9 and S2), their normalized inward current magnitude shown here is overestimated (by greater or equal to threefold; Fig. 9). (E) D935 (green sticks) and E963 (red sticks) are  $\sim 10\text{\AA}$  apart in the *Xenopus*  $\alpha 1\text{Na}^+/\text{K}^+$  pump homology model of the  $\text{E}2 \cdot \text{MgF}_4^{2-}$  conformation (Fig. 3 B), with the hydroxyl of TM5 Y780 (purple sticks) between them; view magnified 2.5 times, from the right-hand image of Fig. 3 B. (F) The response of inward current in Y780F ( $n = 4$ ) mutant pumps to lowering  $\text{pH}_o$  from 7.6 to 6.0.

for purposes of comparison with C113Y. Indeed, assessments of D935N expression levels using transient  $\text{Na}^+$  charge movements or palytoxin-induced currents (see Fig. 9) indicate that the D935N inward currents (Fig. 4 C) are overestimated by about threefold. Given the relative positions of E963 and D935 in the  $\text{Na}^+/\text{K}^+$  pump's TM domain (Fig. 3 B), the apparent requirement of both carboxylates for robust proton inflow that our findings indicate could be explained if extracellular protons bind to E963 and subsequently transfer to D935, from where they access the cytoplasm (compare to Fig. 3 A). Estimates of  $\text{pK}_a$  based on the  $\text{E}2 \cdot \text{MgF}_4^{2-} \cdot 2\text{K}^+ \text{Na}^+/\text{K}^+$  pump crystal structure do imply that E963 and D935 are both protonated in that conformation, and a cytoplasmic route for D935 protonation and deprotonation has been proposed (Poulsen et al., 2010).

However, the E963 and D935 carboxylates are separated by  $\sim 10\text{\AA}$  in the  $\text{K}^+$ -bound  $\text{E}2 \cdot \text{MgF}_4^{2-}$  structure (Fig. 4 E; Shinoda et al., 2009; also in the  $\text{Na}^+$ -bound E1 structure, Kanai et al., 2013). We therefore examined whether the hydroxyl of the intervening tyrosine Y780 might serve to allow proton relay. The inward current increase on lowering  $\text{pH}_o$  to 6.0 was markedly attenuated by the conservative mutation Y780F (Fig. 4 F), which did not affect outward  $\text{Na}^+/\text{K}^+$  currents (Fig. S2 H), confirming that the hydroxyl is also required for proton inflow (Li et al., 2006). In comparison, a substantial amplification of inward current at pH 6.0 was not prevented (Fig. S3) by individual mutation of TM histidines (H292A, H295A, H921A, and H921N; compare to Vasilyev et al., 2004) nor of C-terminal arginine or lysine (R1007N and K1008A), nor by C-terminal truncation ( $\Delta\text{YY}$  and  $\Delta\text{KESYY}$ ). Collectively, these results argue that extracellular protons travel from E963 to Y780 to D935, residues in or near  $\text{Na}^+$ -binding site III (Ogawa and Toyoshima, 2002; Poulsen et al., 2010; Kanai et al., 2013; Nyblom et al., 2013). Near abolition of inward current by a conservative mutation at any one of these three positions demonstrates the absence of alternative, parallel, pathways for net proton flow.

#### The proton route is distinct from the principal pathway for transported $\text{Na}^+$ and $\text{K}^+$ ions

The proton route we infer, between TM9, TM8, TM5, and TM6 (Fig. 3 B), passes through  $\text{Na}^+$  site III (Kanai et al., 2013; Nyblom et al., 2013) and differs from the principal pathway proposed for translocation of pumped  $\text{Na}^+$  and  $\text{K}^+$  ions, between TM1, TM2, TM4, and TM6, passing through site II (Fig. 3 B; Takeuchi et al., 2008). The latter path, evident as a funnel open to the extracytoplasmic side in crystal structures of the related SERCA Ca-ATPase in a  $\text{BeF}_3^-$ -trapped E2P-like conformation

is small, as in D935N or E963Q pumps, compared with that of C113Y pumps.

(Olesen et al., 2007; Toyoshima et al., 2007) and in related  $\text{Na}^+/\text{K}^+$  pump models (Takeuchi et al., 2008), was corroborated by a cysteine scan of TM1–TM6 accessibility to the small positively charged MTS reagent, MTSET<sup>+</sup>, in palytoxin-bound  $\text{Na}^+/\text{K}^+$  pump channels (Reyes and Gadsby, 2006; Takeuchi et al., 2008); palytoxin transforms  $\text{Na}^+/\text{K}^+$  pumps into ion channels by disrupting the coordination between their alternating gates (Artigas and Gadsby, 2003).

Because cytoplasmic-side access to sites I and II is closed in  $\text{BeF}_3^-$ -bound SERCA structures (by a 15–20 Å barrier; Olesen et al., 2007), and  $\text{Na}^+/\text{K}^+$  pump treatment with  $\text{BeF}_X$  prevents channel opening by palytoxin (Takeuchi et al., 2008), to further distinguish the proton route from that taken by pumped  $\text{Na}^+$  and  $\text{K}^+$ , we examined the influence of  $\text{BeF}_X$  on inward proton current.  $\text{BeF}_X$  injection into oocytes (Fig. 5 A) essentially abolished the large  $\text{K}^+$ -activated outward current at positive potentials in C113Y  $\text{Na}^+/\text{K}^+$  pumps (Fig. 5, A and B), but

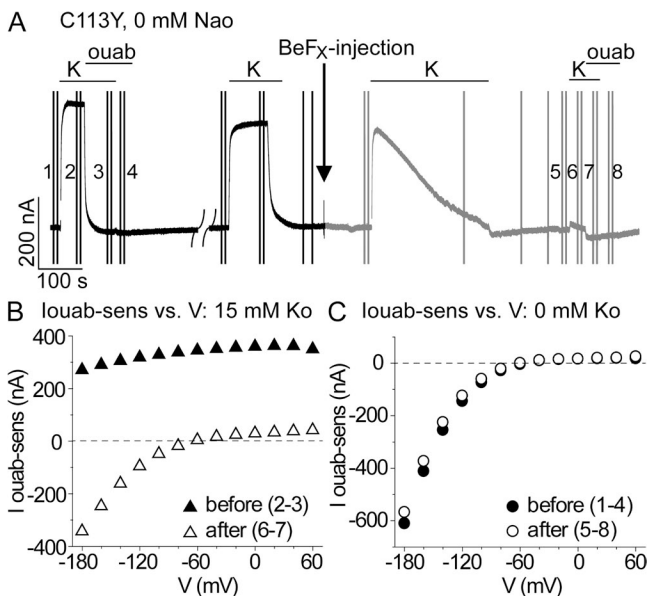


**Figure 5.** Closing the cytoplasmic  $\text{Na}^+$  and  $\text{K}^+$  access pathway in C113Y pumps by using  $\text{BeF}_X$  to restrict them to phosphorylated-like states does not impair inward proton current. (A) Outward current in C113Y  $\text{Na}^+/\text{K}^+$  pumps at -20 mV in  $\text{Na}^+$ -free solution was twice activated by 15 mM  $\text{K}^+$  before online injection of 1 mM  $\text{BeF}_X$  into the oocyte (black downward arrow and gray current recording). The slow current decay in 15 mM  $\text{K}^+$  after  $\text{BeF}_X$  injection reflects accumulation of pumps in stable E2P-like states incapable of  $\text{Na}^+/\text{K}^+$  exchange (Olesen et al., 2007; Toyoshima et al., 2007). The numbers mark the voltage trials used to obtain the subtracted currents shown in B and C. (B and C)  $\text{BeF}_X$  abolished ouabain-sensitive outward current in 15 mM  $\text{K}^+$  at positive voltages (B; open vs. closed triangles) but did not alter inward current in 0  $\text{K}^+$  (C; open vs. closed circles).  $\text{BeF}_X$  also prevented  $\text{K}^+$  inhibition of inward current at negative voltages (B; open vs. closed triangles); two other identical experiments gave the same results, as did nine experiments with C113Y-ΔYY pumps (C-terminal truncation mutant; Vedovato and Gadsby, 2010) in 0  $\text{Na}^+$  ( $n = 6$ ) or in 125 mM  $\text{Na}^+$  ( $n = 3$ ).

inward proton current in  $\text{K}^+$ -free,  $\text{Na}^+$ -free solution remained unaltered (Fig. 5 C). Importantly, after  $\text{Na}^+/\text{K}^+$  pump inhibition by  $\text{BeF}_X$ , presumably by formation of relatively stable E2P-like states with tightly bound  $\text{BeF}_X$ , 15 mM  $\text{K}^+$  failed not only to activate appreciable outward current at positive potentials but also to inhibit inward proton current at negative potentials (Fig. 5 B). This argues that dephosphorylation of E2P, required for  $\text{K}^+$  occlusion and for completion of the  $\text{Na}^+/\text{K}^+$  transport cycle (Fig. 1), is also required for  $\text{K}^+$  to prevent proton inflow. Unaltered inward proton current in  $\text{BeF}_X$ -inhibited  $\text{Na}^+/\text{K}^+$  pumps provides unequivocal evidence that proton import requires only phosphorylated states.

In addition,  $\text{BeF}_X$ -inhibited C113Y  $\text{Na}^+/\text{K}^+$  pumps generated unaltered transient  $\text{Na}^+$  currents in response to voltage steps in 0  $\text{K}^+$ , 125-mM  $\text{Na}^+$  solution (Fig. 6, A and B; Nakao and Gadsby, 1986; Holmgren et al., 2000; Meier et al., 2010; Vedovato and Gadsby, 2010). The asymptotes of the  $\Delta Q$  voltage plots (Fig. 6 C) are attributed to  $\text{Na}^+/\text{K}^+$  pump accumulation in state E2P, with no bound  $\text{Na}^+$ , at positive potentials, and in E2P and E1P states, with three  $\text{Na}^+$  ions bound, at negative potentials (Heyse et al., 1994; Hilgemann, 1994; Holmgren et al., 2000; Gadsby et al., 2012). Moreover, the slow (Fig. 6 D) components of  $\text{Na}^+$  charge movement examined here are believed to be rate limited by the major E1P( $\text{Na}^3$ ) $\leftrightarrow$ E2P( $\text{Na}^2$ ) $\text{Na}$  conformational change (Fig. 1; Heyse et al., 1994; Hilgemann, 1994; Holmgren et al., 2000; Gadsby et al., 2012). These unaltered charge movements therefore demonstrate that  $\text{BeF}_X$ -bound  $\text{Na}^+/\text{K}^+$  pumps are not locked into a single conformational analogue of the E2P ground state (e.g., Cornelius et al., 2013). Rather,  $\text{BeF}_X$ -bound  $\text{Na}^+/\text{K}^+$  pumps are faithful mimics of phosphorylated pumps and, in the presence of  $\text{Na}^+$ , they can adopt all conformations, and can undergo all transitions, of phosphorylated pumps, from E2P to the occluded E1P( $\text{Na}^3$ ) form.

We found previously that modification by MTSET<sup>+</sup> of a cysteine substituted for T806, at the extracellular end of TM6 (Fig. 3 B), abolished the large inward  $\text{Na}^+$  currents ( $>10^6 \text{ Na}^+ \text{ s}^{-1}$  per pump; e.g., Fig. 9) that flow through palytoxin-bound T806C  $\text{Na}^+/\text{K}^+$  pump channels (Reyes and Gadsby, 2006; Takeuchi et al., 2008). We therefore examined whether that modification of the external cation transport pathway would similarly impair inward proton current (Fig. 7). MTSET<sup>+</sup> reaction with T806C (without palytoxin treatment) abolished  $\text{K}^+$ -activated outward  $\text{Na}^+/\text{K}^+$  pump current (C113Y-ΔYY pumps; Fig. 7, A and B), but large inward proton currents persisted (Fig. 7 C, before vs. after), although their voltage dependence was altered somewhat. Strikingly, after MTSET<sup>+</sup> treatment, large inward currents were observed even in the presence of 15 mM  $\text{K}^+$  (Fig. 7 B), implying that MTSET<sup>+</sup> modification of T806C abolishes outward  $\text{Na}^+/\text{K}^+$  pump current by interfering with the binding and occlusion of  $\text{K}^+$  ions. These results with MTSET<sup>+</sup> further

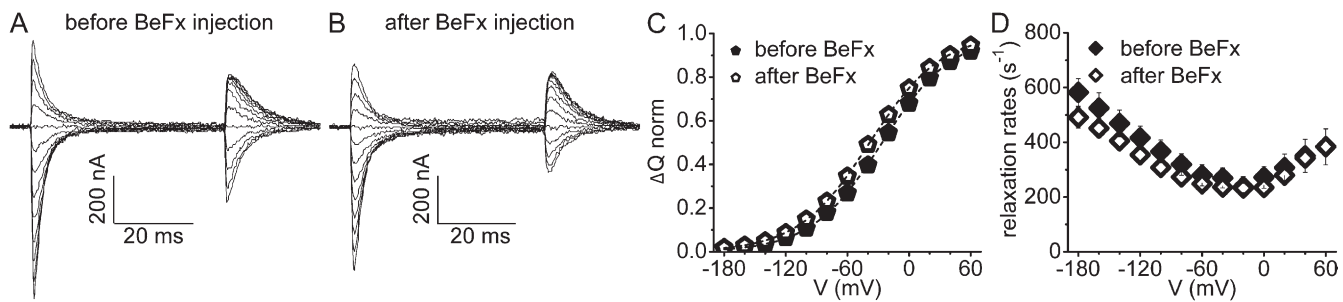


**Figure 6.** BeFx-bound  $\text{Na}^+/\text{K}^+$  pumps mimic conformational transitions of normal phosphorylated pumps. (A and B) C113Y  $\text{Na}^+/\text{K}^+$  pump-mediated pre-steady-state  $\text{Na}^+$  charge movements (e.g., Nakao and Gadsby, 1986; Meier et al., 2010; Vedovato and Gadsby, 2010) elicited by steps from -20 mV to potentials between -180 and +60 mV, in 125 mM  $\text{Na}^+_{\text{o}}$ , 0  $\text{K}^+_{\text{o}}$  before (A) and after (B) oocyte injection with 1 mM BeFx (as in Fig. 5 A). (C) Ouabain-sensitive charge,  $\Delta Q$ , on termination of each step is plotted against step voltage, and  $\Delta Q$ -V is fitted with the Boltzmann relation to determine total charge moved,  $Q_{\text{tot}}$ , effective valence,  $z_q$ , and midpoint voltage; none was altered by BeFx injection. The ratio of  $Q_{\text{tot}}$  before versus after BeFx was 1.2 for A and B, and averaged  $1.1 \pm 0.1$  ( $n = 3$ ). The same results were obtained with C113Y- $\Delta$ YY mutants ( $Q_{\text{tot}}$  ratio =  $1.15 \pm 0.02$ ;  $n = 4$ ). In contrast, the ratio of  $\text{K}^+_{\text{o}}$ -activated outward pump current after versus before BeFx injection was  $\leq 0.2$  for C113Y pumps (e.g., outward current was reduced by 88% for the oocyte of A and B, and by  $\sim 90\%$  for C113Y- $\Delta$ YY pumps). (D) Mean ( $n = 3$ ) relaxation rates of the transient currents elicited by the ON voltage steps, plotted against voltage, were not altered by BeFx. The unaltered transient  $\text{Na}^+$  charge movements demonstrate that BeFx-bound and inhibited  $\text{Na}^+/\text{K}^+$  pumps remain capable of a subset of normal conformational changes in 125-mM  $\text{Na}^+_{\text{o}}$  solutions.

substantiate our above conclusion that the protons travel a pathway distinct from that used by the preponderance of transported  $\text{Na}^+$  and  $\text{K}^+$  ions.

#### Proton inflow results from back-steps during $\text{Na}^+/\text{K}^+$ transport

We chose absence of  $\text{K}^+_{\text{o}}$  and  $\text{Na}^+_{\text{o}}$  as the experimental condition in the above tests to emphasize the contribution

of the inward proton current and thus facilitate its characterization. But does net proton influx occur only in the absence of  $\text{K}^+_{\text{o}}$ , as generally stated (Rakowski et al., 1991; Efthymiadis et al., 1993; Wang and Horisberger, 1995; Vasilyev et al., 2004; Li et al., 2006; Yaragatupalli et al., 2009; Meier et al., 2010; Poulsen et al., 2010; Ratheal et al., 2010; Vedovato and Gadsby, 2010; Nyblom et al., 2013), or does it also happen at physiological  $\text{Na}^+$  and

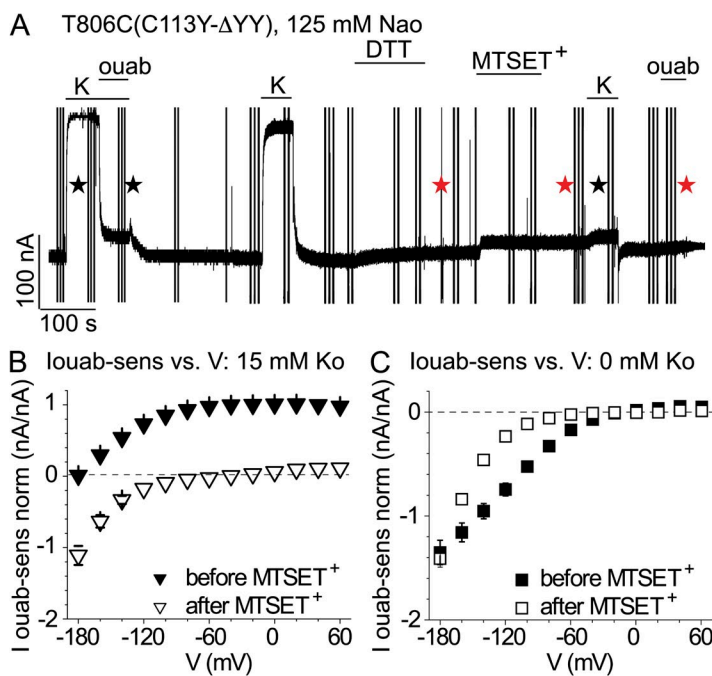


**Figure 7.** Preventing extracellular access to the principal  $\text{Na}^+$  and  $\text{K}^+$  transport pathway does not impair inward proton current in C113Y- $\Delta$ YY  $\text{Na}^+/\text{K}^+$  pumps. (A) Recording of abolition by 1 mM MTSET<sup>+</sup> of  $\text{K}^+_{\text{o}}$ -activated outward current in T806C(C113Y- $\Delta$ YY) mutant  $\text{Na}^+/\text{K}^+$  pumps, at -50 mV in 125-mM  $\text{Na}^+_{\text{o}}$  solutions; the  $\Delta$ YY mutant was chosen as background because that C-terminal truncation amplifies proton currents in 125 mM  $\text{Na}^+_{\text{o}}$  (Yaragatupalli et al., 2009; Poulsen et al., 2010; Vedovato and Gadsby, 2010), the condition in which MTSET<sup>+</sup> abolished large  $\text{Na}^+$  currents in palytoxin-bound  $\text{Na}^+/\text{K}^+$  pump channels (Reyes and Gadsby, 2006; Takeuchi et al., 2008). 10 mM dithiothreitol (bar labeled "DTT") was first applied to reverse any spontaneous cysteine oxidation. Outward pump current was assessed before and after the modification by MTSET<sup>+</sup> (bar labeled "MTSET<sup>+</sup>"). Black and red stars, respectively, mark voltage trials that typically yielded the average subtracted currents shown in B (at 15 mM  $\text{K}^+_{\text{o}}$ ) and C (at 0  $\text{K}^+_{\text{o}}$ ). (B) Ouabain-sensitive currents were normalized to the outward pump current between 0 and +60 mV in 15 mM  $\text{K}^+_{\text{o}}$  before MTSET<sup>+</sup> in each oocyte, and then averaged. In 15 mM  $\text{K}^+_{\text{o}}$ , outward current at positive voltages was reduced by  $90 \pm 0.02\%$  ( $n = 7$  oocytes) by MTSET<sup>+</sup>, but current was inward at large negative potentials, indicating that  $\text{K}^+_{\text{o}}$  could no longer inhibit inward proton current. (C) Inward currents in 0  $\text{K}^+_{\text{o}}$  were normalized to the ouabain-sensitive outward current between 0 and +60 mV in 15 mM  $\text{K}^+_{\text{o}}$  before MTSET<sup>+</sup> in each oocyte, and then averaged. MTSET<sup>+</sup> modification of T806C did not diminish inward current amplitude at -180 mV ( $n = 7$  oocytes), although voltage sensitivity was altered.

$K^+$  concentrations? If so, does it accompany normal  $Na^+/K^+$  transport, and might it even be obligatory for  $Na^+/K^+$  exchange? To address these questions, we determined current generated by wild-type  $Na^+/K^+$  pumps (i.e., over-expressed *Xenopus*  $\alpha 1/\beta 3$ ) exposed to 125 mM  $Na^+_{\text{o}}$  both with 0  $K^+_{\text{o}}$  and with 15 mM  $K^+_{\text{o}}$ , all at  $pH_{\text{o}}$  7.6 (as in Fig. 2, A–C), and then repeated the measurements at  $pH_{\text{o}}$  6.0 (Fig. 8, A and B). Without  $K^+_{\text{o}}$ , inward current at negative potentials was small but measurable at  $pH_{\text{o}}$  7.6 (Fig. 8 B, closed squares; see Fig. S4 A for mean data), and was considerably amplified at  $pH$  6.0 (Figs. 8 B and S4 A, open squares), qualitatively similar to the large amplification of inward current observed on lowering  $pH_{\text{o}}$  to 6.0 in the same wild-type pumps in 0  $Na^+_{\text{o}}$  (Fig. 2 D).

But with 15 mM  $K^+_{\text{o}}$ , the asymptotic outward currents at positive potentials were identical at  $pH_{\text{o}}$  7.6 and 6.0 (Fig. 8 B, closed vs. open stars), showing that pumps reach the same maximal  $Na^+/K^+$  transport rate (i.e., forward cycle rate,  $\sim 45 \text{ s}^{-1}$ ) regardless of  $pH_{\text{o}}$  level, and hence that proton current is absent at the most positive

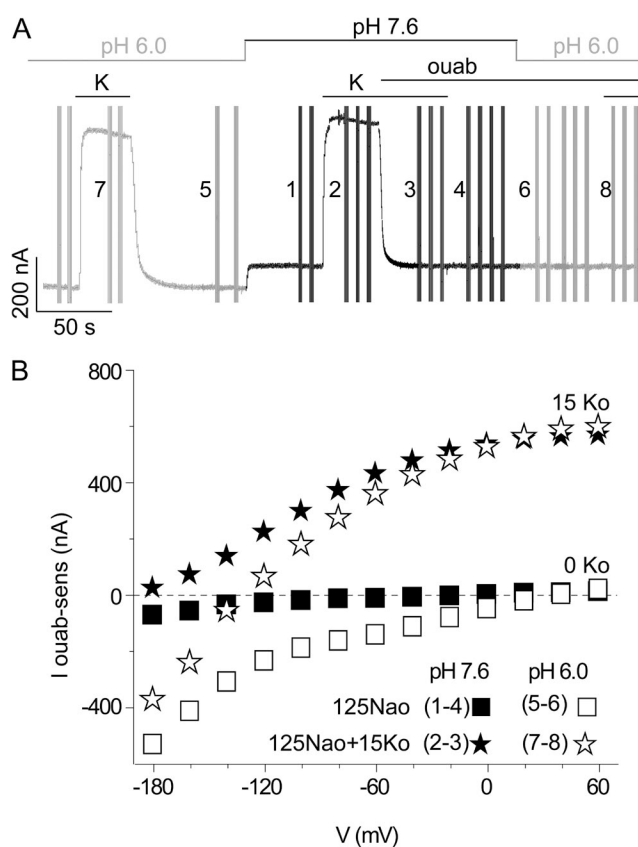


**Figure 8.** Wild-type  $Na^+/K^+$  pump currents in 125 mM  $Na^+_{\text{o}}$  at normal and lowered  $pH_{\text{o}}$ . (A) Current record at  $-20 \text{ mV}$  (same oocyte as in Fig. 2, A and B) during the addition of 15 mM  $K^+_{\text{o}}$  and ouabain, as indicated, at  $pH_{\text{o}}$  6.0 (gray current trace) and  $pH_{\text{o}}$  7.6 (black trace). (B) Ouabain-sensitive steady currents without (squares) and with (stars) 15 mM  $K^+_{\text{o}}$ , at  $pH_{\text{o}}$  7.6 (closed symbols) and 6.0 (open symbols), from subtraction of currents in numbered voltage trials in A (the same results obtained in  $n = 8$  oocytes are shown averaged in Fig. S4 A).

voltages (proton current is also absent at positive potentials in 0  $K^+_{\text{o}}$ ; Fig. 8 B, closed vs. open squares). Proton influx is therefore not obligatory for  $Na^+/K^+$  exchange. At potentials more negative than  $-120 \text{ mV}$ , ouabain-sensitive current in 15 mM  $K^+_{\text{o}}$  remains outward at  $pH_{\text{o}}$  7.6 (Fig. 8 B, closed stars) but is net inward at  $pH_{\text{o}}$  6.0 (Fig. 8 B, open stars). Reversal of the 3  $Na^+/2 K^+$  transport cycle (Fig. 1) is thermodynamically infeasible under these conditions, because the  $Na^+/K^+$  pump equilibrium potential (e.g., Veech et al., 1979; Tanford, 1981; De Weer et al., 1988) is estimated to be at least as negative as  $-240 \text{ mV}$  under physiological conditions (and even more negative at the elevated  $[K^+_{\text{o}}]$  and  $[Na^+_{\text{i}}]$  of these experiments), and it is not expected to vary with  $pH_{\text{o}}$ . All  $Na^+/K^+$  transport current must therefore be outward over the entire voltage range explored here. Thus, the net inward current measured at extreme negative voltage means that the inward proton current generated by the entire population of  $Na^+/K^+$  pumps exceeds any outward  $Na^+/K^+$  exchange current being generated by that pump population at the same time. As that same population of pumps generates only outward current at positive potentials under these conditions (15 mM  $K^+_{\text{o}}$  at  $pH_{\text{o}}$  6.0), if we assume the pumps are all identical, then each pump must be capable of generating both outward  $Na^+/K^+$  transport current and inward proton current. A pump must complete a forward (clockwise) step through every transition in the  $Na^+/K^+$  transport cycle (Fig. 1) to generate net outward current, but it needs to visit only the phosphorylated subset of states in that cycle (Figs. 5 and 6) to generate inward proton current (Fig. 5, B and C). We therefore conclude that each pump may generate both inward proton current and outward  $Na^+/K^+$  current during the same transport cycle. Moreover, proton current prevalence at more negative voltages, where completion of the forward  $Na^+/K^+$  transport cycle slows (and outward current thus declines), suggests that proton inflow results from reversal of a step that is a normal participant in  $Na^+/K^+$  transport; i.e., reversal of a transition between phosphorylated states.

Near  $-120 \text{ mV}$ , where net current is zero in 15 mM  $K^+_{\text{o}}$  at  $pH_{\text{o}}$  6.0 in this oocyte (Fig. 8 B, open stars), outward  $Na^+/K^+$  exchange current must just balance inward proton current; i.e., on average, a single proton enters the cell through every  $Na^+/K^+$  pump during each complete  $Na^+/K^+$  transport cycle. In other words, at  $-120 \text{ mV}$  and  $pH_{\text{o}}$  6.0, approximately one proton-importing back-step occurs in each cycle before  $K^+_{\text{o}}$  binding triggers E2P dephosphorylation and  $K^+$  occlusion, thereby preventing any further proton inflow in that 3  $Na^+/2 K^+$  transport cycle. At the most negative membrane potentials, each complete  $Na^+/K^+$  transport cycle at  $pH_{\text{o}}$  6.0 must on average include multiple reiterations of the proton-importing back-step (perhaps as many as 10 at  $-180 \text{ mV}$  in this example, from comparison of the

amplitude of outward current in 15 mM  $K^+$ o at pH<sub>o</sub> 7.6 [Fig. 8 B, closed stars] with that of the net inward current in 15 mM  $K^+$ o at pH<sub>o</sub> 6.0 [open stars]). Even between −60 and 0 mV, outward current in 15 mM  $K^+$ o is somewhat smaller at pH<sub>o</sub> 6.0 (Fig. 8 B, open stars) than at pH<sub>o</sub> 7.6 (closed stars), indicating that, also at modest negative potentials, in every  $Na^+/K^+$  pump an occasional proton-importing back-step interrupts forward progression of the normal  $Na^+/K^+$  transport cycle at pH<sub>o</sub> 6.0. At −80 mV, a value between the resting potentials of cardiac and skeletal muscle (−90 mV), and those of neurons (−60 to −70 mV), the normalized (to maximal outward current, corresponding to ∼45 cycles s<sup>−1</sup>) inward proton current in 0 mM  $K^+$ o, 125 mM  $Na^+$ o at pH<sub>o</sub> 7.6 (Figs. 8 B and S4 A, closed squares) averaged  $−0.025 \pm 0.003$  ( $n = 8$ ), corresponding to ∼1 proton entry s<sup>−1</sup>, and at pH<sub>o</sub> 6.0 (Figs. 8 B and S4 A, open squares) was  $−0.287 \pm 0.009$  ( $n = 8$ ), corresponding to ∼13 protons entered s<sup>−1</sup>. Because outward pump current at −80 mV and at pH<sub>o</sub> 7.6 (Fig. 8 B, closed stars) corresponded to ∼30  $Na^+/K^+$  exchange cycles s<sup>−1</sup>, we can conclude that, even under these relatively physiological conditions, on average one proton enters the cell through each  $Na^+/K^+$  pump every ∼30 transport cycles. The results for C113Y  $Na^+/K^+$  pumps were qualitatively similar to the findings in wild-type *Xenopus*  $Na^+/K^+$  pumps (Fig. S4, A vs. B), except that inward currents, and hence proton inflow rates, were consistently larger in the C113Y pumps, as noted previously for both C113Y and RD ouabain-resistant pumps (Vedovato and Gadsby, 2010).

## DISCUSSION

### Normalization procedures for reliable comparison of $Na^+/K^+$ pump mutants

To allow for differences in expression of the same  $Na^+/K^+$  pumps from oocyte to oocyte, and to permit meaningful comparisons between wild-type and mutant  $Na^+/K^+$  pumps, it was important to establish reliable procedures for normalizing pump-generated currents and to validate them with estimates of numbers of functional pumps. Relative magnitudes and voltage sensitivities of currents mediated by wild-type or mutant pumps under various conditions are well preserved by normalization to the amplitude of outward  $Na^+/K^+$  transport current at positive potentials and saturating [K<sup>+</sup>o] measured in the same oocyte (i.e., to maximal turnover conditions); in practice (Figs. 4, S1, and S2), we normalized to the average current between 0 and +60 mV because, in wild-type and C113Y parent pumps, outward current is constant over that range. But to calculate molecular turnover rates for inward and/or outward pump currents—even in E336Q and D813N pumps that generate no K<sup>+</sup>o-activated current (although both show robust amplification of inward current on lowering pH<sub>o</sub> to 6.0)—we used

Boltzmann fits to measured transient  $Na^+$  charge movements to determine the total charge moved,  $Q_{tot}$ , and hence to estimate the number of pumps in the oocyte surface (as described in Results). Although, strictly, two-state Boltzmann fits yield accurate estimates of  $Q_{tot}$  only when the charge moves in a single step (Chowdhury and Chanda, 2012; Bezanilla and Villalba-Galea, 2013), that is likely to be a reasonable assumption in this instance. Thus, the slow component of charge measured here is rate limited by the single step E1P(Na3)↔E2P(Na2)Na (Heyse et al., 1994; Hilgemann, 1994; Holmgren et al., 2000; Gadsby et al., 2012), and it amounts to ∼95% of the total moved in the three steps associated with release/rebinding of the three  $Na^+$  ions (Gadsby et al., 2012). In addition, we limited estimation of turnover rates to only those mutants for which  $z_q$  values were little altered.

The maximal voltage-independent turnover rate at saturating [K<sup>+</sup>o] of C113Y α1 *Xenopus* pumps determined in this way in these experiments was  $18 \pm 1$  s<sup>−1</sup> ( $n = 13$ ). As reported previously, this is identical to that of RD α1 *Xenopus* pumps and wild-type rat (RD) α1 pumps, and roughly half that of wild-type α1/β3 *Xenopus* pumps (Vedovato and Gadsby, 2010). This maximal turnover rate was unaltered in E788Q ( $18 \pm 1$  s<sup>−1</sup>;  $n = 11$ ) and E963Q ( $17 \pm 0.1$  s<sup>−1</sup>;  $n = 7$ ) pumps, but the turnover rate at 0 mV was diminished approximately threefold in D935N ( $6 \pm 0.2$  s<sup>−1</sup>;  $n = 11$ ) and D935N/E963Q ( $7 \pm 1$  s<sup>−1</sup>;  $n = 4$ ) pumps, and was zero in E336Q and D813N pumps. The  $\Delta Q$ -voltage plots for these six mutants had  $Q_{tot}$ ,  $z_q$ , and midpoint voltage values comparable to those of C113Y, but were somewhat shallower and shifted, by ∼30 mV positive for D817N and by ∼30 mV negative for Y780F, precluding reliable Boltzmann fits and hence turnover rate estimates for those mutants. The principal consequence of using the charge movement values to convert the inward current data at 0  $Na^+$ o, 0  $K^+$ o, and pH<sub>o</sub> 6.0 in Fig. 4 to rates, therefore, is diminution of the relative proton import rates of D935N and D935N/E963Q pumps to 12 and 3%, respectively, of parent C113Y proton transport rates under those same conditions.

To further corroborate the diminished  $Na^+/K^+$  transport rates of D935N pumps, we exploited the ability of palytoxin to readily transform even mutant pumps into cation channels (e.g., E336C, D813C, D817C; Reyes and Gadsby, 2006), and made side-by-side comparison of palytoxin-induced current in excised patches and  $Na^+/K^+$  pump current at saturating [K<sup>+</sup>o] in intact oocytes injected with the same amount of cRNA encoding either C113Y or D935N pumps (Fig. 9). Palytoxin-induced currents had the same amplitude in patches containing C113Y pumps as in patches containing D935N pumps after 1 d, and after 2 d (when the currents were twice as large), of expression (Fig. 9, A and B). In contrast, however, in the same oocytes after 2 d of expression, outward  $Na^+/K^+$  transport current at 0 mV was almost

fourfold smaller for D935N than for C113Y pumps (Fig. 9, C and D). The same-sized palytoxin-induced currents (D935N,  $-2.1 \pm 0.1$  nA and  $n = 8$ ; C113Y,  $-2.1 \pm 0.2$  nA and  $n = 15$ ) suggest that the surface densities of D935N and of C113Y pumps are the same; this assumes that the D935N mutation has little influence over the single-channel conductance or open probability of palytoxin-bound pump channels (observed to be  $\geq 0.9$  in the presence of mM ATP, as used here, for all palytoxin-bound pump channels examined to date; e.g., Artigas and Gadsby, 2003, 2006). That the surface expression levels of D935N and C113Y pumps are indeed similar is also suggested by the similar total charge movements recorded after expression of the same amounts of cRNA for the same time:  $Q_{\text{tot}}$  for D935N =  $8.5 \pm 0.5$  nC,  $n = 5$ ;  $Q_{\text{tot}}$  for C113Y =  $9.3 \pm 1.2$  nC,  $n = 13$ . These similar  $Q_{\text{tot}}$ , and corresponding  $z_q$ , values, determined in the same experiments that yielded the D935N and C113Y outward  $\text{Na}^+/\text{K}^+$  transport currents in Fig. S2 B, resulted in the approximately threefold smaller turnover rate at 0 mV estimated for D935N compared with C113Y pumps, corroborating the impaired pump function of D935N pumps (Einholt et al., 2010; Poulsen et al., 2010).

#### Structural underpinnings of proton translocation mechanism

SERCA  $\text{Ca}^{2+}$ -ATPases pump out two cytosolic  $\text{Ca}^{2+}$  and countertransport two to three protons per cycle (Yu et al., 1993). But close proximity of binding-site oxygens demands protonation of at least two carboxylates, even with two  $\text{Ca}^{2+}$  ions bound in sites I and II (Sugita et al., 2005). Similarly, pKa calculations on  $\text{K}^+$ -bound  $\text{E2} \cdot \text{MgF}_4^{2-}$ - $\text{Na}^+/\text{K}^+$ -ATPase suggest that three site I and II carboxylates, equivalent to E336, E788, and D817 (Figs. 3 B and 4, A and B), as well as carboxylates D935 and E963 near site III (Figs. 3 B and 4, C and E), all examined here, are

protonated in that conformation (Poulsen et al., 2010; Yu et al., 2011). In fact, disengagement of the  $\text{Na}^+/\text{K}^+$  pump's C terminus, thus uncovering an aqueous pathway that permits D935 protonation from the cytoplasm, was proposed (Poulsen et al., 2010) to rate limit the  $\text{E1P}(\text{Na}3) \rightarrow \text{E2P}(\text{Na}2)\text{Na}$  deocclusion transition and hence extracellular release of the first of the three  $\text{Na}^+$  ions. That proton was suggested to return to the cytoplasm after intracellular  $\text{K}^+$  ion release to allow binding of the next three intracellular  $\text{Na}^+$  ions (Poulsen et al., 2010). We propose here that once site III becomes vacant upon extracellular release of the first  $\text{Na}^+$  (whether that  $\text{Na}^+$  leaves from site II followed by lateral shuffling of the two remaining  $\text{Na}^+$ , or leaves directly from site III), an extracellular proton may bind to E963, within 10 Å of that empty site, and then relay via Y780 to D935 from where it can access the cytoplasm via the aqueous pathway. The hydroxyl of that tyrosine might stabilize a hydrogen-bonded water chain, enabling fast proton transfer by a Grothuss-type mechanism, as in cytochrome *c* oxidase (Backgren et al., 2000). In such cases, the dynamics of proton translocation reflect the time taken for waters to enter and establish the chain. Indeed, a bound water bridges E963 and Y780 equivalents in both the  $\text{K}^+$ -containing  $\text{E2} \cdot \text{MgF}_4^{2-}$  structure (Shinoda et al., 2009) and the recent 2.8-Å resolution structure of  $\text{E1} \cdot \text{AlF}_4^- \cdot \text{ADP} \cdot 3 \text{Na}^+$ , which contains three  $\text{Na}^+$  ions (Kanai et al., 2013). A 4.3-Å resolution structure of the same  $\text{E1} \cdot \text{AlF}_4^- \cdot \text{ADP} \cdot 3 \text{Na}^+$  conformation (Nyblom et al., 2013) also locates the third  $\text{Na}^+$  between TM8, TM5, and TM6, coordinated by D935 equivalent, in the site previously called IIIb (Poulsen et al., 2010). It was recently suggested that the originally proposed third  $\text{Na}^+$  site, containing E963 and Y780 equivalents (Ogawa and Toyoshima, 2002; Li et al., 2005), which has been referred to as site IIIa (Poulsen et al., 2010), might be a

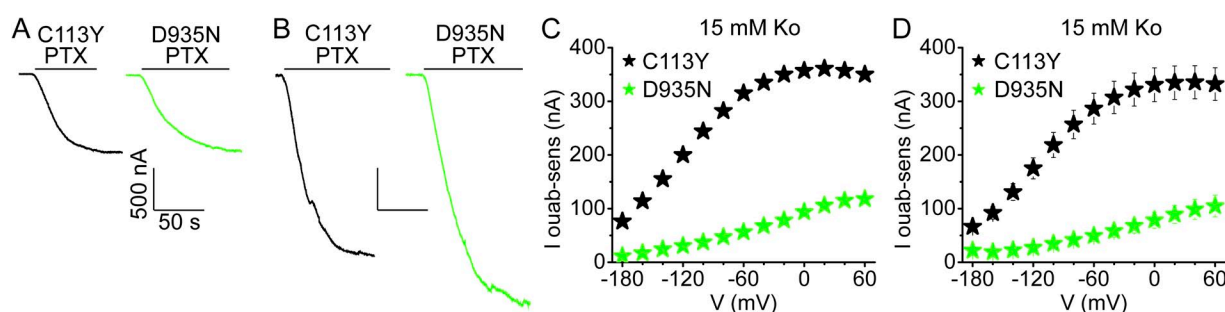


**Figure 9.** Comparing expression and function of D935N (C113Y) and parent C113Y pumps. (A and B) Representative recordings of pump-channel currents induced by 100 nM palytoxin (PTX), at  $-50$  mV with symmetrical 125-mM  $[\text{Na}^+]$  solutions, in outside-out patches excised from oocytes injected with the same amounts of cRNA (30 ng  $\alpha$  subunit plus 10 ng  $\beta$  subunit): (A) after 1 d of expression (black, C113Y: steady current amplitude,  $-1.2 \pm 0.2$  nA and  $n = 4$ ; green, D935N:  $-1.1 \pm 0.2$  nA and  $n = 4$ ), and (B) after 2 d (black, C113Y:  $-2.1 \pm 0.2$  nA and  $n = 15$ ; green, D935N:  $-2.1 \pm 0.1$  nA and  $n = 8$ ). (C) Ouabain-sensitive outward  $\text{Na}^+/\text{K}^+$  transport currents at 15 mM  $\text{K}_o$  in 125 mM  $\text{Na}_o$  from the very same two C113Y-expressing (black stars) and D35N-expressing (green stars) oocytes from which the patch recordings in B were obtained. (D) Average outward pump currents in 15 mM  $\text{K}_o$  and 125 mM  $\text{Na}_o$  for C113Y (black stars;  $n = 12$ ) and D935N (green stars;  $n = 9$ ) after 2 d of expression, recorded in oocytes (including those of B and C) from the same batches that yielded the average excised-patch data in B.

transient site for extracellular  $\text{Na}^+$  release/rebinding (Nyblom et al., 2013); it was also suggested, in accord with the findings presented here, to be a site where extracellular protons might bind and then transfer to the site previously called IIIb and escape to the cytoplasm, generating inward current (Nyblom et al., 2013).

It is not yet possible to specify precisely the phosphorylated states involved in proton import or pinpoint the high activation energy transitions between them that rate limit proton inflow. But the responsible step must have relatively high transition rates (relative to the rate-limiting  $\text{K}^+$  deocclusion step) because, at large negative membrane potentials and low  $\text{pH}_o$ , multiple proton-importing back-steps seem to occur in each completed (albeit slowed)  $3 \text{ Na}^+ / 2 \text{ K}^+$  cycle (Fig. 8 B). Analyses of the three sequential steps responsible for extracellular release of the three  $\text{Na}^+$  show that after the slowest step,  $\text{E1P}(\text{Na}3) \rightarrow \text{E2P}(\text{Na}2)\text{Na}$ , enables release of the first  $\text{Na}^+$ , deocclusion and release of the second and third  $\text{Na}^+$  ions occur relatively rapidly (Heyse et al., 1994; Hilgemann, 1994; Holmgren et al., 2000; Gadsby et al., 2012). The rates of all  $\text{Na}^+$ -releasing steps after the slow  $\text{E1P} \rightarrow \text{E2P}$  conformational change therefore seem appropriate for allowing several forward and reverse transitions, importing several protons, before the binding of two  $\text{K}^+$  ions prompts dephosphorylation, precluding further proton entry. Raising the external proton concentration enhances proton inflow whether  $\text{K}^+$  and/or  $\text{Na}^+$  are present or absent (e.g., Figs. 2 D and 8), although to a greater extent when both are absent (Fig. 2 D); presumably, lowered  $\text{pH}_o$  raises the probability of the extracellularly accessible E963 being protonated and so increases the frequency of the proton-importing back-step. The similar magnitudes of the inward current increments at negative potentials caused by lowering  $\text{pH}_o$  to 6.0 in 125 mM  $\text{Na}^+$ , whether  $\text{K}^+$  is present (15 mM) or absent (Fig. 8 B), support that interpretation, but they also imply that, at least in the presence of  $\text{Na}^+$ , the steady-state fractional occupancy of the phosphorylated conformation involved in accepting an extracellular proton is independent of that of the  $\text{K}^+$ -occluded conformation. This relatively constant occupancy of the proton-accepting conformation in 125 mM  $\text{Na}^+$  might be explained if, under those conditions, it were a high energy state with a short lifetime, determined by fast transition rates in either direction, as proposed previously (Hilgemann, 1994) to account for characteristics of the major electrogenic  $\text{Na}^+$  release that follows the slow  $\text{E1P} \rightarrow \text{E2P}$  deocclusion.

The observed inhibition of proton current by extracellular  $\text{Na}^+$  (e.g., Fig. 2 C; 125 vs. 0 mM  $\text{Na}^+$ ; Efthymiadis et al., 1993; Wang and Horisberger, 1995; Vasilyev et al., 2004) could reflect direct competition between  $\text{Na}^+$  ions and external protons for binding to E963 (e.g., if the first  $\text{Na}^+$  is released directly from site III), or  $\text{Na}^+$ -mediated redistribution of  $\text{Na}^+/\text{K}^+$  pump states and hence

destabilization of the proton-accepting conformation. The latter is more consistent with the recent structural interpretation of single-file binding of three  $\text{Na}^+$  ions from the cytoplasm (Kanai et al., 2013) and earlier indications of strictly sequential, last-in first-out, external release of two  $\text{K}^+$  ions (Forbush, 1987b) and three  $\text{Na}^+$  ions (Wuddel and Apell, 1995; Wagg and Gadsby, 1997). Because the new structure suggests that the last cytoplasmic  $\text{Na}^+$  resides in site II (Kanai et al., 2013), external release of that  $\text{Na}^+$  via the principal pathway between TM1, TM2, TM4, and TM6 would allow site III to be vacated by lateral hops of the two residual  $\text{Na}^+$ , enabling proton inflow. In the absence of  $\text{Na}^+$ , site III would remain vacant and proton inflow would continue. But in the presence of  $\text{Na}^+$ , rebinding of  $\text{Na}^+$  to site II would allow occupancy of site I, and thence, occasionally, site III, with resulting temporary interruption of proton inflow.  $\text{K}^+$  ions, if present, would occupy sites I and II (readily, in the absence of competition from  $\text{Na}^+$ , and eventually, in its presence) and trigger dephosphorylation, precluding proton inflow.

By the same token, modified responses to  $\text{Na}^+$  of the inward currents in mutant pumps might reflect altered distribution of pump states or altered interactions with  $\text{Na}^+$ , or both. Altered consequences of changes in extracellular concentration of  $\text{Na}^+$  or  $\text{Na}^+$  substitutes have contributed to suggestions that cations other than protons might carry the inward current through wild-type or mutant pumps (Vasilyev et al., 2004; Yaragatupalli et al., 2009; Meier et al., 2010; Poulsen et al., 2010; Ratheal et al., 2010; Azizan et al., 2013; Nyblom et al., 2013). In no case, however, has modification of proton current caused by redistribution of pump states been ruled out. In particular, the strong inward rectification of the proton current makes measurements of its reversal potential problematic for both wild-type and mutant pumps, and appropriate weighting of small inward current differences observed in mutants will require accurate normalization for numbers of pumps, using methods like those introduced here.

#### Physiological/pathophysiological implications

This work establishes that, even in the presence of physiological  $\text{K}^+$  and  $\text{Na}^+$  concentrations, when  $\text{Na}^+/\text{K}^+$  pumps hesitate in E2P states, after releasing the first  $\text{Na}^+$  ion but before binding and occluding  $\text{K}^+$  ions—for example, at negative potentials that strengthen effective competition between  $\text{Na}^+$  and  $\text{K}^+$  ions—a reverse transition in the cycle can import a proton. Proton inflow occurs at measurable rates when  $[\text{H}^+]_o$  is elevated (Figs. 2 D and 8 B; compare to Efthymiadis et al., 1993; Wang and Horisberger, 1995), so pump-mediated proton delivery to the cytoplasm must be considered a possible consequence of  $\text{Na}^+/\text{K}^+$  pump exposure to low extracytoplasmic pH. Interestingly, activity of endocytosed  $\text{Na}^+/\text{K}^+$  pumps has been reported to limit  $\text{H}^+$ -ATPase acidification of

early endosomes to pH ≥6, as treatment with ouabain was found to further lower endosomal pH to ≤5.5 (Cain et al., 1989; Fuchs et al., 1989; Zen et al., 1992). Although H<sup>+</sup>-ATPase slowing by a more positive endosome interior as a result of electrogenic Na<sup>+</sup>/K<sup>+</sup> transport was initially proposed as the mechanism (Fuchs et al., 1989), direct Na<sup>+</sup>/K<sup>+</sup> pump-mediated flow of protons from endosome interior to cytoplasm now provides a reasonable alternative explanation.

Moreover, in human skeletal muscle, extracellular pH is known to fall rapidly during vigorous exercise (from 7.4 to below 7.0 in 5 min, and still falling; Street et al., 2001), and is lowered because of poor perfusion in tumors (Gillies et al., 1994) and during ischemia in the brain (Vorísek and Syková, 1997) or heart (Yan and Kléber, 1992). Although proton import rates per pump may be relatively low (Fig. 8 B), Na<sup>+</sup>/K<sup>+</sup> pump densities in muscle, nerve, and heart can be very high ( $\geq 1,000 \mu\text{m}^{-2}$ ; Nakao and Gadsby, 1986; Anderson et al., 2010). It seems plausible, therefore, that if negative resting potentials are maintained (as measurements in working skeletal muscle imply; Street et al., 2001), and if pH<sub>o</sub> becomes low enough, proton inflow might become significant. For example, in rabbit heart papillary muscle, ischemia lowered pH<sub>o</sub> from 7.4 to an average of 6.46 in 18 min (Yan and Kléber, 1992), and a pH<sub>o</sub> drop from 7.4 to 6.4 resulted in acidification of the interior of guinea pig cardiac myocytes by  $\sim 0.1 \text{ pH units min}^{-1}$  (Sun et al., 1996). Depending on whether the buffer power inside myocytes is taken as 15 mM/pH unit (Bountra et al., 1990) or 60 mM/pH unit (Vaughan-Jones et al., 2009), the observed acidification rate requires a net proton influx of 1.5–6 mM H<sup>+</sup> min<sup>-1</sup>, some 80–85% of which was reported to be mediated by two Cl<sup>-</sup>-dependent anion exchangers (Sun et al., 1996); in that case, only the remainder, 0.3–1.2 mM H<sup>+</sup> min<sup>-1</sup>, could possibly enter a myocyte via Na<sup>+</sup>/K<sup>+</sup> pumps. As Na<sup>+</sup>/K<sup>+</sup> pump-mediated Na<sup>+</sup> efflux in myocytes beating at 1 Hz is  $\sim 3.5 \text{ mM min}^{-1}$  (e.g., Bers et al., 2003), pump-mediated proton entry of 0.3–1.2 mM H<sup>+</sup> min<sup>-1</sup> would require a proton to enter every fourth Na<sup>+</sup>/K<sup>+</sup> transport cycle to once every cycle when pH<sub>o</sub> is 6.4. Our results (Fig. 8 B) indeed show that, at a membrane potential of  $-80 \text{ mV}$ , outward Na<sup>+</sup>/K<sup>+</sup> pump-mediated current in 15 mM K<sup>+</sup> and 125 mM Na<sup>+</sup> at pH 7.6 (closed stars) becomes smaller by about one quarter when pH<sub>o</sub> is lowered to 6.0 (open stars). Assuming that the smaller net outward pump current is entirely attributable to increased inward proton current (e.g., compare open with closed squares in Fig. 8 B) summed with unaltered outward Na<sup>+</sup>/K<sup>+</sup> transport current, the implication is that on average, one proton enters the oocyte every four Na<sup>+</sup>/K<sup>+</sup> transport cycles under these conditions (i.e., pH<sub>o</sub> 6.0). Our data suggest that even at pH<sub>o</sub> 7.6, one proton enters every 25–30 pump cycles at  $-80 \text{ mV}$  (Fig. 8 B, closed squares vs. closed stars). As most of the myocyte and

oocyte data compared here were gathered at room temperature, extrapolation to more physiological conditions should be undertaken only with caution. For at least that reason, it seems safe to conclude that whether Na<sup>+</sup>/K<sup>+</sup> pump-mediated proton uptake plays any physiological or pathological role remains to be established.

#### Na<sup>+</sup>/K<sup>+</sup>-ATPase: A hybrid transporter?

These results show that the Na<sup>+</sup>/K<sup>+</sup>-ATPase can behave as a mixed function, or hybrid, transporter, exporting three Na<sup>+</sup> and importing two K<sup>+</sup> uphill in each ATPase cycle, during which it may also import one or more protons downhill. Other examples of hybrid transporters (Gadsby, 2009) include members of the human excitatory amino acid transporter (EAAT) family. These transporters, in addition to carrying out Na<sup>+</sup>-coupled stoichiometric glutamate uptake, generate Cl<sup>-</sup> ion currents that are activated by substrate binding but are energetically uncoupled from its transport (Fairman et al., 1995; Vandenberg et al., 2008). The Cl<sup>-</sup> ion pathway exists in only a subset of the conformations visited during the substrate transport cycle (Wadiche and Kavanaugh, 1998). A potential structural correlate of the anion-conducting state was recently identified in an intermediate conformation of a prokaryotic homologue (Verdon and Boudker, 2012) as a crevice between the very mobile transport domain and the static trimerization scaffold domain (Reyes et al., 2009). So the Cl<sup>-</sup> current might reasonably be viewed as the unavoidable byproduct of the evolution of a structure and a mechanism that efficiently cotransports Na<sup>+</sup> and glutamate. However, variation in the relationship between substrate transport rate and Cl<sup>-</sup> current amplitude among EAAT isoforms (Wadiche et al., 1995; Vandenberg et al., 2008), with correlated variation in their physiological role (Veruki et al., 2006; Tzingounis and Wadiche, 2007), implies selective modulation by evolution of the stability and/or physicochemical characteristics of the conformation(s) underlying the Cl<sup>-</sup> current. Similarly, the possibility that, at sufficiently low pH<sub>o</sub>, protons may traverse the Na<sup>+</sup>/K<sup>+</sup> pump to reach the cytoplasm can be viewed as the price paid by evolution for efficient export of three Na<sup>+</sup> and import of two K<sup>+</sup> across the cell membrane. But whether, like EAAT-mediated Cl<sup>-</sup> current, Na<sup>+</sup>/K<sup>+</sup> pump-mediated proton inflow varies among isoforms of Na<sup>+</sup>/K<sup>+</sup>-ATPase  $\alpha$  and/or  $\beta$  subunits, or is subject to regulation, has yet to be explored.

We thank the late R.F. Rakowski for *Xenopus*  $\alpha 1$  and  $\beta 3$  Na<sup>+</sup>, K<sup>+</sup>-ATPase cDNAs, A. Gulyás-Kovács for writing acquisition and analysis software, P. Hoff for preparing oocytes, N. Fataliev for molecular biological support, and Mauro Caffarelli for help in preliminary experiments.

This work was supported by National Institutes of Health grant HL36783 to D.C. Gadsby.

The authors declare no competing financial interests.

Merritt C. Maduke served as editor.

Submitted: 11 December 2013  
Accepted: 13 February 2014

## REFERENCES

Anderson, T.R., J.R. Huguenard, and D.A. Prince. 2010. Differential effects of  $\text{Na}^+/\text{K}^+$  ATPase blockade on cortical layer V neurons. *J. Physiol.* 588:4401–4414. <http://dx.doi.org/10.1113/jphysiol.2010.191858>

Artigas, P., and D.C. Gadsby. 2003.  $\text{Na}^+/\text{K}^+$ -pump ligands modulate gating of palytoxin-induced ion channels. *Proc. Natl. Acad. Sci. USA.* 100:501–505. <http://dx.doi.org/10.1073/pnas.0135849100>

Artigas, P., and D.C. Gadsby. 2006. Ouabain affinity determining residues lie close to the  $\text{Na}/\text{K}$  pump ion pathway. *Proc. Natl. Acad. Sci. USA.* 103:12613–12618. <http://dx.doi.org/10.1073/pnas.0602720103>

Azizan, E.A.B., H. Poulsen, P. Tuluc, J. Zhou, M.V. Clausen, A. Lieb, C. Maniero, S. Garg, E.G. Bochukova, W. Zhao, et al. 2013. Somatic mutations in ATP1A1 and CACNA1D underlie a common subtype of adrenal hypertension. *Nat. Genet.* 45:1055–1060. <http://dx.doi.org/10.1038/ng.2716>

Backgren, C., G. Hummer, M. Wikström, and A. Puustinen. 2000. Proton translocation by cytochrome c oxidase can take place without the conserved glutamic acid in subunit I. *Biochemistry.* 39:7863–7867. <http://dx.doi.org/10.1021/bi000806b>

Bahinski, A., M. Nakao, and D.C. Gadsby. 1988. Potassium translocation by the  $\text{Na}^+/\text{K}^+$  pump is voltage insensitive. *Proc. Natl. Acad. Sci. USA.* 85:3412–3416. <http://dx.doi.org/10.1073/pnas.85.10.3412>

Bers, D.M., W.H. Barry, and S. Despa. 2003. Intracellular  $\text{Na}^+$  regulation in cardiac myocytes. *Cardiovasc. Res.* 57:897–912. [http://dx.doi.org/10.1016/S0008-6363\(02\)00656-9](http://dx.doi.org/10.1016/S0008-6363(02)00656-9)

Bezanilla, F., and C.A. Villalba-Galea. 2013. The gating charge should not be estimated by fitting a two-state model to a Q-V curve. *J. Gen. Physiol.* 142:575–578. <http://dx.doi.org/10.1085/jgp.201311056>

Bountra, C., T. Powell, and R.D. Vaughan-Jones. 1990. Comparison of intracellular pH transients in single ventricular myocytes and isolated ventricular muscle of guinea-pig. *J. Physiol.* 424:343–365.

Burnay, M., G. Crampert, S. Kharoubi-Hess, K. Geering, and J.-D. Horisberger. 2003. Electrogenicity of  $\text{Na},\text{K}$ - and  $\text{H},\text{K}$ -ATPase activity and presence of a positively charged amino acid in the fifth transmembrane segment. *J. Biol. Chem.* 278:19237–19244. <http://dx.doi.org/10.1074/jbc.M300946200>

Cain, C.C., D.M. Sipe, and R.F. Murphy. 1989. Regulation of endocytic pH by the  $\text{Na}^+/\text{K}^+$ -ATPase in living cells. *Proc. Natl. Acad. Sci. USA.* 86:544–548. <http://dx.doi.org/10.1073/pnas.86.2.544>

Canessa, C.M., J.-D. Horisberger, D. Louvard, and B.C. Rossier. 1992. Mutation of a cysteine in the first transmembrane segment of  $\text{Na},\text{K}$ -ATPase  $\alpha$  subunit confers ouabain resistance. *EMBO J.* 11:1681–1687.

Chowdhury, S., and B. Chanda. 2012. Estimating the voltage-dependent free energy change of ion channels using the median voltage for activation. *J. Gen. Physiol.* 139:3–17. <http://dx.doi.org/10.1085/jgp.201110722>

Cornelius, F., R. Kanai, and C. Toyoshima. 2013. A structural view on the functional importance of the sugar moiety and steroid hydroxyls of cardiotonic steroids in binding to  $\text{Na},\text{K}$ -ATPase. *J. Biol. Chem.* 288:6602–6616. <http://dx.doi.org/10.1074/jbc.M112.442137>

De Weer, P., D.C. Gadsby, and R.F. Rakowski. 1988. Voltage dependence of the  $\text{Na},\text{K}$  pump. *Annu. Rev. Physiol.* 50:225–241. <http://dx.doi.org/10.1146/annurev.physiol.50.1.225>

De Weer, P., D.C. Gadsby, and R.F. Rakowski. 2001. Voltage dependence of the apparent affinity for external  $\text{Na}^+$  of the backward-running sodium pump. *J. Gen. Physiol.* 117:315–328. <http://dx.doi.org/10.1085/jgp.117.4.315>

DeCoursey, T.E. 2003. Voltage-gated proton channels and other proton transfer pathways. *Physiol. Rev.* 83:475–579.

Efthymiadis, A., J. Rettinger, and W. Schwarz. 1993. Inward-directed current generated by the  $\text{Na}^+/\text{K}^+$  pump in  $\text{Na}^+$ - and  $\text{K}^+$ -free medium. *Cell Biol. Int.* 17:1107–1116. <http://dx.doi.org/10.1006/cbir.1993.1043>

Einholm, A.P., M.S. Toustrup-Jensen, R. Holm, J.P. Andersen, and B. Vilsen. 2010. The rapid-onset dystonia parkinsonism mutation D923N of the  $\text{Na}^+/\text{K}^+$ -ATPase  $\alpha 3$  isoform disrupts  $\text{Na}^+$  interaction at the third  $\text{Na}^+$  site. *J. Biol. Chem.* 285:26245–26254. <http://dx.doi.org/10.1074/jbc.M110.123976>

Fairman, W.A., R.J. Vandenberg, J.L. Arriza, M.P. Kavanaugh, and S.G. Amara. 1995. An excitatory amino-acid transporter with properties of a ligand-gated chloride channel. *Nature.* 375:599–603. <http://dx.doi.org/10.1038/375599a0>

Forbush, B., III. 1987a. Rapid release of  $42\text{K}$  and  $86\text{Rb}$  from an occluded state of the  $\text{Na},\text{K}$ -pump in the presence of ATP or ADP. *J. Biol. Chem.* 262:11104–11115.

Forbush, B., III. 1987b. Rapid release of  $42\text{K}$  or  $86\text{Rb}$  from two distinct transport sites on the  $\text{Na},\text{K}$ -pump in the presence of Pi or vanadate. *J. Biol. Chem.* 262:11116–11127.

Fuchs, R., S. Schmid, and I. Mellman. 1989. A possible role for  $\text{Na}^+/\text{K}^+$ -ATPase in regulating ATP-dependent endosome acidification. *Proc. Natl. Acad. Sci. USA.* 86:539–543. <http://dx.doi.org/10.1073/pnas.86.2.539>

Gadsby, D.C. 2009. Ion channels versus ion pumps: the principal difference, in principle. *Nat. Rev. Mol. Cell Biol.* 10:344–352. <http://dx.doi.org/10.1038/nrm2668>

Gadsby, D.C., R.F. Rakowski, and P. De Weer. 1993. Extracellular access to the  $\text{Na},\text{K}$  pump: Pathway similar to ion channel. *Science.* 260:100–103. <http://dx.doi.org/10.1126/science.7682009>

Gadsby, D.C., F. Bezanilla, R.F. Rakowski, P. De Weer, and M. Holmgren. 2012. The dynamic relationships between the three events that release individual  $\text{Na}^+$  ions from the  $\text{Na}^+/\text{K}^+$ -ATPase. *Nat. Commun.* 3:669. <http://dx.doi.org/10.1038/ncomms1673>

Garrahan, P.J., and I.M. Glynn. 1967a. The stoichiometry of the sodium pump. *J. Physiol.* 192:217–235.

Garrahan, P.J., and I.M. Glynn. 1967b. The incorporation of inorganic phosphate into adenosine triphosphate by reversal of the sodium pump. *J. Physiol.* 192:237–256.

Gillies, R.J., Z. Liu, and Z. Bhujwalla. 1994. 31P-MRS measurements of extracellular pH of tumors using 3-aminopropylphosphonate. *Am. J. Physiol.* 267:C195–C203.

Good, P.J., K. Richter, and I.B. Dawid. 1990. A nervous system-specific isotype of the  $\beta$  subunit of  $\text{Na}^+/\text{K}^+$ -ATPase expressed during early development of *Xenopus laevis*. *Proc. Natl. Acad. Sci. USA.* 87:9088–9092. <http://dx.doi.org/10.1073/pnas.87.23.9088>

Heyse, S., I. Wuddel, H.-J. Apell, and W. Stürmer. 1994. Partial reactions of the  $\text{Na},\text{K}$ -ATPase: Determination of rate constants. *J. Gen. Physiol.* 104:197–240. <http://dx.doi.org/10.1085/jgp.104.2.197>

Hilgemann, D.W. 1994. Channel-like function of the  $\text{Na},\text{K}$  pump probed at microsecond resolution in giant membrane patches. *Science.* 263:1429–1432. <http://dx.doi.org/10.1126/science.8128223>

Holmgren, M., J. Wagg, F. Bezanilla, R.F. Rakowski, P. De Weer, and D.C. Gadsby. 2000. Three distinct and sequential steps in the release of sodium ions by the  $\text{Na}^+/\text{K}^+$ -ATPase. *Nature.* 403:898–901. <http://dx.doi.org/10.1038/35002599>

Kanai, R., H. Ogawa, B. Vilsen, F. Cornelius, and C. Toyoshima. 2013. Crystal structure of a  $\text{Na}^+$ -bound  $\text{Na}^+/\text{K}^+$ -ATPase preceding the E1P state. *Nature.* 502:201–206. <http://dx.doi.org/10.1038/nature12578>

Koenderink, J.B., S. Geibel, E. Grabsch, J.J. De Pont, E. Bamberg, and T. Friedrich. 2003. Electrophysiological analysis of the mutated  $\text{Na},\text{K}$ -ATPase cation binding pocket. *J. Biol. Chem.* 278:51213–51222. <http://dx.doi.org/10.1074/jbc.M306384200>

Law, R.J., K. Munson, G. Sachs, and F.C. Lightstone. 2008. An ion gating mechanism of gastric  $\text{H},\text{K}$ -ATPase based on molecular dynamics simulations. *Biophys. J.* 95:2739–2749. <http://dx.doi.org/10.1529/biophysj.107.128025>

Li, C., O. Capendeguy, K. Geering, and J.-D. Horisberger. 2005. A third  $\text{Na}^+$ -binding site in the sodium pump. *Proc. Natl. Acad. Sci. USA.* 102:12706–12711. <http://dx.doi.org/10.1073/pnas.0505980102>

Li, C., K. Geering, and J.-D. Horisberger. 2006. The third sodium binding site of  $\text{Na},\text{K}$ -ATPase is functionally linked to acidic pH-activated inward current. *J. Membr. Biol.* 213:1–9. <http://dx.doi.org/10.1007/s00232-006-0035-0>

Meier, S., N.N. Tavraz, K.L. Dürr, and T. Friedrich. 2010. Hyperpolarization-activated inward leakage currents caused by deletion or mutation of carboxy-terminal tyrosines of the  $\text{Na}^+/\text{K}^+$ -ATPase  $\alpha$  subunit. *J. Gen. Physiol.* 135:115–134. <http://dx.doi.org/10.1085/jgp.200910301>

Morth, J.P., B.P. Pedersen, M.S. Toustrup-Jensen, T.L. Sørensen, J. Petersen, J.P. Andersen, B. Vilzen, and P. Nissen. 2007. Crystal structure of the sodium-potassium pump. *Nature.* 450:1043–1049. <http://dx.doi.org/10.1038/nature06419>

Nakao, M., and D.C. Gadsby. 1986. Voltage dependence of  $\text{Na}^+$  translocation by the  $\text{Na}/\text{K}$  pump. *Nature.* 323:628–630. <http://dx.doi.org/10.1038/323628a0>

Nakao, M., and D.C. Gadsby. 1989.  $[\text{Na}]$  and  $[\text{K}]$  dependence of the  $\text{Na}/\text{K}$  pump current–voltage relationship in guinea pig ventricular myocytes. *J. Gen. Physiol.* 94:539–565. <http://dx.doi.org/10.1085/jgp.94.3.539>

Nielsen, J.M., P.A. Pedersen, S.J. Karlsh, and P.L. Jorgensen. 1998. Importance of intramembrane carboxylic acids for occlusion of  $\text{K}^+$  ions at equilibrium in renal  $\text{Na},\text{K}$ -ATPase. *Biochemistry.* 37:1961–1968. <http://dx.doi.org/10.1021/bi972524q>

Nyblom, M., H. Poulsen, P. Gourdon, L. Reinhard, M. Andersson, E. Lindahl, N. Fedosova, and P. Nissen. 2013. Crystal structure of  $\text{Na}^+$ ,  $\text{K}^+$ -ATPase in the  $\text{Na}^+$ -bound state. *Science.* 342:123–127. <http://dx.doi.org/10.1126/science.1243352>

Obara, K., N. Miyashita, C. Xu, I. Toyoshima, Y. Sugita, G. Inesi, and C. Toyoshima. 2005. Structural role of countertransport revealed in  $\text{Ca}^{2+}$  pump crystal structure in the absence of  $\text{Ca}^{2+}$ . *Proc. Natl. Acad. Sci. USA.* 102:14489–14496. <http://dx.doi.org/10.1073/pnas.0506222102>

Ogawa, H., and C. Toyoshima. 2002. Homology modeling of the cation binding sites of  $\text{Na}^+/\text{K}^+$ -ATPase. *Proc. Natl. Acad. Sci. USA.* 99:15977–15982. <http://dx.doi.org/10.1073/pnas.202622299>

Olesen, C., M. Picard, A.M. Winther, C. Gyurp, J.P. Morth, C. Oxvig, J.V. Møller, and P. Nissen. 2007. The structural basis of calcium transport by the calcium pump. *Nature.* 450:1036–1042. <http://dx.doi.org/10.1038/nature06418>

Peluffo, R.D., J.M. Argüello, and J.R. Berlin. 2000. The role of  $\text{Na},\text{K}$ -ATPase  $\alpha$  subunit serine 775 and glutamate 779 in determining the extracellular  $\text{K}^+$  and membrane potential–dependent properties of the  $\text{Na},\text{K}$ -pump. *J. Gen. Physiol.* 116:47–60. <http://dx.doi.org/10.1085/jgp.116.1.47>

Post, R.L., and P.C. Jolly. 1957. The linkage of sodium, potassium, and ammonium active transport across the human erythrocyte membrane. *Biochim. Biophys. Acta.* 25:118–128. [http://dx.doi.org/10.1016/0006-3002\(57\)90426-2](http://dx.doi.org/10.1016/0006-3002(57)90426-2)

Post, R.L., C. Hegváry, and S. Kume. 1972. Activation by adenosine triphosphate in the phosphorylation kinetics of sodium and potassium ion transport adenosine triphosphatase. *J. Biol. Chem.* 247:6530–6540.

Poulsen, H., H. Khandelia, J.P. Morth, M. Bublitz, O.G. Mouritsen, J. Egebjerg, and P. Nissen. 2010. Neurological disease mutations compromise a C-terminal ion pathway in the  $\text{Na}^+/\text{K}^+$ -ATPase. *Nature.* 467:99–102. <http://dx.doi.org/10.1038/nature09309>

Rakowski, R.F., D.C. Gadsby, and P. De Weer. 1989. Stoichiometry and voltage dependence of the sodium pump in voltage-clamped, internally dialyzed squid giant axon. *J. Gen. Physiol.* 93:903–941. <http://dx.doi.org/10.1085/jgp.93.5.903>

Rakowski, R.F., L.A. Vasilets, J. LaTona, and W. Schwarz. 1991. A negative slope in the current–voltage relationship of the  $\text{Na}^+/\text{K}^+$  pump in *Xenopus* oocytes produced by reduction of external  $[\text{K}^+]$ . *J. Membr. Biol.* 121:177–187. <http://dx.doi.org/10.1007/BF01870531>

Ratheal, I.M., G.K. Virgin, H. Yu, B. Roux, C. Gatto, and P. Artigas. 2010. Selectivity of externally facing ion-binding sites in the  $\text{Na}/\text{K}$  pump to alkali metals and organic cations. *Proc. Natl. Acad. Sci. USA.* 107:18718–18723. <http://dx.doi.org/10.1073/pnas.1004214107>

Reyes, N., and D.C. Gadsby. 2006. Ion permeation through the  $\text{Na}^+/\text{K}^+$ -ATPase. *Nature.* 443:470–474. <http://dx.doi.org/10.1038/nature05129>

Reyes, N., C. Ginter, and O. Boudker. 2009. Transport mechanism of a bacterial homologue of glutamate transporters. *Nature.* 462:880–885. <http://dx.doi.org/10.1038/nature08616>

Sagar, A., and R.F. Rakowski. 1994. Access channel model for the voltage dependence of the forward-running  $\text{Na}^+/\text{K}^+$  pump. *J. Gen. Physiol.* 103:869–893. <http://dx.doi.org/10.1085/jgp.103.5.869>

Schneeberger, A., and H.-J. Apell. 2001. Ion selectivity of the cytoplasmic binding sites of the  $\text{Na},\text{K}$ -ATPase: II. Competition of various cations. *J. Membr. Biol.* 179:263–273. <http://dx.doi.org/10.1007/s002320010051>

Shinoda, T., H. Ogawa, F. Cornelius, and C. Toyoshima. 2009. Crystal structure of the sodium-potassium pump at 2.4 Å resolution. *Nature.* 459:446–450. <http://dx.doi.org/10.1038/nature07939>

Starace, D.M., and F. Bezanilla. 2001. Histidine scanning mutagenesis of basic residues of the S4 segment of the *Shaker K<sup>+</sup>* channel. *J. Gen. Physiol.* 117:469–490. <http://dx.doi.org/10.1085/jgp.117.5.469>

Street, D., J. Bangsbo, and C. Juel. 2001. Interstitial pH in human skeletal muscle during and after dynamic graded exercise. *J. Physiol.* 537:993–998. <http://dx.doi.org/10.1113/jphysiol.2001.012954>

Sugita, Y., N. Miyashita, M. Ikeguchi, A. Kidera, and C. Toyoshima. 2005. Protonation of the acidic residues in the transmembrane cation-binding sites of the  $\text{Ca}^{2+}$  pump. *J. Am. Chem. Soc.* 127:6150–6151. <http://dx.doi.org/10.1021/ja0427505>

Sun, B., C.H. Leem, and R.D. Vaughan-Jones. 1996. Novel chloride-dependent acid loader in the guinea-pig ventricular myocyte: part of a dual acid-loading mechanism. *J. Physiol.* 495:65–82.

Takeuchi, A., N. Reyes, P. Artigas, and D.C. Gadsby. 2008. The ion pathway through the opened  $\text{Na}^+/\text{K}^+$ -ATPase pump. *Nature.* 456:413–416. <http://dx.doi.org/10.1038/nature07350>

Tanford, C. 1981. Equilibrium state of ATP-driven ion pumps in relation to physiological ion concentration gradients. *J. Gen. Physiol.* 77:223–229. <http://dx.doi.org/10.1085/jgp.77.2.223>

Toyoshima, C., Y. Norimatsu, S. Iwasawa, T. Tsuda, and H. Ogawa. 2007. How processing of aspartylphosphate is coupled to luminal gating of the ion pathway in the calcium pump. *Proc. Natl. Acad. Sci. USA.* 104:19831–19836. <http://dx.doi.org/10.1073/pnas.0709978104>

Tzingounis, A.V., and J.I. Wadiche. 2007. Glutamate transporters: confining runaway excitation by shaping synaptic transmission. *Nat. Rev. Neurosci.* 8:935–947. <http://dx.doi.org/10.1038/nrn2274>

Vandenberg, R.J., S. Huang, and R.M. Ryan. 2008. Slips, leaks and channels in glutamate transporters. *Channels (Austin).* 2:51–58. <http://dx.doi.org/10.4161/chan.2.1.6047>

Vasilyev, A., K. Khater, and R.F. Rakowski. 2004. Effect of extracellular pH on presteady-state and steady-state current mediated by the  $\text{Na}^+/\text{K}^+$  pump. *J. Membr. Biol.* 198:65–76. <http://dx.doi.org/10.1007/s00232-004-0660-4>

Vaughan-Jones, R.D., K.W. Spitzer, and P. Swietach. 2009. Intracellular pH regulation in heart. *J. Mol. Cell. Cardiol.* 46:318–331. <http://dx.doi.org/10.1016/j.jmcc.2008.10.024>

Vedovato, N., and D.C. Gadsby. 2010. The two C-terminal tyrosines stabilize occluded  $\text{Na}/\text{K}$  pump conformations containing  $\text{Na}$  or  $\text{K}$  ions. *J. Gen. Physiol.* 136:63–82. <http://dx.doi.org/10.1085/jgp.201010407>

Veech, R.L., J.W. Lawson, N.W. Cornell, and H.A. Krebs. 1979. Cytosolic phosphorylation potential. *J. Biol. Chem.* 254:6538–6547.

Verdon, G., and O. Boudker. 2012. Crystal structure of an asymmetric trimer of a bacterial glutamate transporter homolog. *Nat. Struct. Mol. Biol.* 19:355–357. <http://dx.doi.org/10.1038/nsmb.2233>

Verrey, F., P. Kairouz, E. Schaeerer, P. Fuentes, K. Geering, B.C. Rossier, and J.P. Kraehenbuhl. 1989. Primary sequence of *Xenopus laevis* Na<sup>+</sup>-K<sup>+</sup>-ATPase and its localization in A6 kidney cells. *Am. J. Physiol.* 256:F1034–F1043.

Veruki, M.L., S.H. Mørkve, and E. Hartveit. 2006. Activation of a presynaptic glutamate transporter regulates synaptic transmission through electrical signaling. *Nat. Neurosci.* 9:1388–1396. <http://dx.doi.org/10.1038/nn1793>

Vilsen, B., and J.P. Andersen. 1998. Mutation to the glutamate in the fourth membrane segment of Na<sup>+</sup>,K<sup>+</sup>-ATPase and Ca<sup>2+</sup>-ATPase affects cation binding from both sides of the membrane and destabilizes the occluded enzyme forms. *Biochemistry*. 37:10961–10971. <http://dx.doi.org/10.1021/bi9802925>

Vorísek, I., and E. Syková. 1997. Ischemia-induced changes in the extracellular space diffusion parameters, K<sup>+</sup>, and pH in the developing rat cortex and corpus callosum. *J. Cereb. Blood Flow Metab.* 17:191–203. <http://dx.doi.org/10.1097/00004647-199702000-00009>

Wadiche, J.I., and M.P. Kavanaugh. 1998. Macroscopic and microscopic properties of a cloned glutamate transporter/chloride channel. *J. Neurosci.* 18:7650–7661.

Wadiche, J.I., S.G. Amara, and M.P. Kavanaugh. 1995. Ion fluxes associated with excitatory amino acid transport. *Neuron*. 15:721–728. [http://dx.doi.org/10.1016/0896-6273\(95\)90159-0](http://dx.doi.org/10.1016/0896-6273(95)90159-0)

Wagg, J., and D.C. Gadsby. 1997. Ordered interaction of ions with Na/K-pump may confound interpretation of unidirectional fluxes. *Ann. NY Acad. Sci.* 834:426–431. <http://dx.doi.org/10.1111/j.1749-6632.1997.tb52290.x>

Wang, X., and J.-D. Horisberger. 1995. A conformation of Na<sup>+</sup>-K<sup>+</sup> pump is permeable to proton. *Am. J. Physiol.* 268:C590–C595.

Wuddel, I., and H.-J. Apell. 1995. Electrogenicity of the sodium transport pathway in the Na,K-ATPase probed by charge-pulse experiments. *Biophys. J.* 69:909–921. [http://dx.doi.org/10.1016/S0006-3495\(95\)79965-9](http://dx.doi.org/10.1016/S0006-3495(95)79965-9)

Yan, G.X., and A.G. Kléber. 1992. Changes in extracellular and intracellular pH in ischemic rabbit papillary muscle. *Circ. Res.* 71:460–470. <http://dx.doi.org/10.1161/01.RES.71.2.460>

Yaragatupalli, S., J.F. Olivera, C. Gatto, and P. Artigas. 2009. Altered Na<sup>+</sup> transport after an intracellular  $\alpha$ -subunit deletion reveals strict external sequential release of Na<sup>+</sup> from the Na/K pump. *Proc. Natl. Acad. Sci. USA*. 106:15507–15512. <http://dx.doi.org/10.1073/pnas.0903752106>

Yu, H., I.M. Ratheal, P. Artigas, and B. Roux. 2011. Protonation of key acidic residues is critical for the K<sup>+</sup>-selectivity of the Na/K pump. *Nat. Struct. Mol. Biol.* 18:1159–1163. <http://dx.doi.org/10.1038/nsmb.2113>

Yu, X., S. Carroll, J.L. Rigaud, and G. Inesi. 1993. H<sup>+</sup> countertransport and electrogenicity of the sarcoplasmic reticulum Ca<sup>2+</sup> pump in reconstituted proteoliposomes. *Biophys. J.* 64:1232–1242. [http://dx.doi.org/10.1016/S0006-3495\(93\)81489-9](http://dx.doi.org/10.1016/S0006-3495(93)81489-9)

Zen, K., J. Biwersi, N. Periasamy, and A.S. Verkman. 1992. Second messengers regulate endosomal acidification in Swiss 3T3 fibroblasts. *J. Cell Biol.* 119:99–110. <http://dx.doi.org/10.1083/jcb.119.1.99>